

Trabalho de Graduação

**Performance Analysis of a Circular Statistics Based
Filter for Pedestrian Indoor Tracking
With Bearings Only Measurements Provided
By Low Cost Sensors**

Vinícius Ferreira Nery

Brasília, dezembro de 2018

UNIVERSIDADE DE BRASÍLIA

FACULDADE DE TECNOLOGIA

UNIVERSIDADE DE BRASÍLIA
Faculdade de Tecnologia

Trabalho de Graduação

**Performance Analysis of a Circular Statistics Based
Filter for Pedestrian Indoor Tracking
With Bearings Only Measurements Provided
By Low Cost Sensors**

Vinícius Ferreira Nery

*Relatório submetido ao Departamento de Engenharia
Elétrica como requisito parcial para obtenção
do grau de Bacharel em Engenharia Elétrica*

Banca Examinadora

Prof. João Yoshiyuki Ishihara, ENE/UnB
Orientador

Prof. Renato Alves Borges, ENE/UnB
Examinador interno

Prof. Henrique Cezar Ferreira, ENE/UnB
Examinador interno

Dedicatória

*À minha mãe Telmara, ao meu pai Francisco, aos meus irmãos, à minha madrinha Edna,
ao meu padrinho Filho e aos meus avós.*

Vinícius Ferreira Nery

Agradecimentos

Agradeço primeiramente aos meus pais, que sempre me deram apoio e me acompanharam por toda a minha caminhada. Agradeço também aos meus irmãos, que sempre estiveram lá me apoiando, fosse para me fazer rir ou me irritar. Agradeço também aos meus amigos que também são minha família: Tchelo, Duds, Gabriel, Luísa, George (Chile), Arthur, Henrique, Brunos e muitos outros que não consegui citar aqui pelo apoio nos momentos bons e ruins. Agradeço imensamente à Nathália que foi meu maior apoio nessa reta final. Agradeço também aos amigos que fiz no curso por caminharem junto comigo sempre me levantando pra cima. Dentre esses posso mencionar Igor, Ricardo, Gabriel, Gian, Heitor, Cid, Caio, e a lista segue. E por fim, mas não menos importante, gostaria de agradecer ao professor Ishihara pela paciência e pelas valorosas discussões e conselhos para que conseguisse finalizar este trabalho.

Vinícius Ferreira Nery

ABSTRACT

Recent literature suggests that circular statistics presents itself as a powerful tool in filtering algorithms that involve angular quantities, allowing a correct treatment of their distributions. In this context, this work aims to provide a performance analysis of a circular statistics based filter algorithm for indoor pedestrian tracking. The measurements for the localization scheme are provided by low cost sensors based on direction of arrival (DOA) techniques. Hence, a correct treatment to the uncertainty of the measurements will be addressed. Simulation experiments carried out in MATLAB indicate that the presented filter outperforms EKF and UKF approaches when the uncertainty is high. Therefore, results inspire the use of the presented filter for physical implementations.

RESUMO

A literatura recente sugere que a estatística circular se apresenta uma ferramenta valiosa em algoritmos de filtragem que envolvem quantidades angulares, permitindo um tratamento correto das distribuições dessas. Nesse contexto, esse trabalho almeja proporcionar uma análise da performance de um de um algoritmo de filtragem, baseado em estatística circular, para rastreamento de pedestres em ambientes fechados. As medidas para o esquema de localização são oriundas de um sensor de baixo custo baseado em técnicas de direção de chegada (DOA). Dessa forma, um tratamento correto da incerteza nas medidas será abordado. Simulações realizadas no MATLAB indicam que o filtro apresentado possui, quando a incerteza é alta, uma performance superior à abordagens que utilizam EKF e UKF. Portanto, os resultados inspiram o uso do filtro apresentado para implementações físicas.

Summary

1	INTRODUCTION	1
1.1	MOTIVATION	1
1.2	PROBLEM STATEMENT	2
1.3	OUTLINE	3
2	TOPICS IN CIRCULAR STATISTICS	4
2.1	THE UNIT CIRCLE	4
2.2	CIRCULAR DATA	5
2.3	CIRCULAR PROBABILITY DISTRIBUTIONS	5
2.3.1	CIRCULAR MODELS	6
2.3.2	WRAPPED NORMAL	6
2.3.3	VON MISES OR CIRCULAR NORMAL	7
2.3.4	WRAPPED DIRAC MIXTURE	9
2.4	TRIGONOMETRIC MOMENTS	9
2.5	CIRCULAR CENTRAL LIMIT THEOREM	10
2.5.1	CENTRAL LIMIT THEOREM	10
2.5.2	CIRCULAR EQUIVALENT	11
3	TOPICS IN ESTIMATION AND FILTERING ALGORITHMS	12
3.1	ESTIMATION THEORY	12
3.1.1	MAXIMUM LIKELIHOOD	12
3.1.2	BAYESIAN ESTIMATION	13
3.2	FILTERING ALGORITHMS	13
3.2.1	PREREQUISITES	13
3.2.2	KALMAN FILTER	15
3.2.3	NONLINEAR FILTERING	17
3.2.4	CIRCULAR FILTERING	22
4	DIRECTION OF ARRIVAL	28
4.1	UNIFORM LINEAR ARRAY	28
4.2	DOA ESTIMATION METHOD	30
4.3	IMPLEMENTATION	30
4.3.1	REPRODUCING PREVIOUS IMPLEMENTATION	31

5	SIMULATION MODELS	34
5.1	MEASUREMENT EQUATION	34
5.2	PEDESTRIAN MOTION	36
5.2.1	LAVEGIN MODEL	36
5.2.2	CONSTANT VELOCITY MODEL	37
6	SIMULATION RESULTS	39
6.1	ANGULAR DISTRIBUTION	39
6.2	ENVIRONMENT	41
6.3	LINEAR KALMAN FILTER APPROACH	41
6.3.1	POSITIONING THE SENSORS	42
6.3.2	FILTER PERFORMANCE	45
6.4	EKF AND UKF APPROACHES	47
6.5	COMPARISON OF THE FILTERS PERFORMANCES	49
7	CONCLUDING REMARKS	51
7.1	FUTURE WORK	51
	BIBLIOGRAPHY	53

List of Figures

1.1	Visualization of the stated problem to be approached.	2
2.1	Three-dimensional representation of a wrapped normal distribution.	7
2.2	Three-dimensional representation of a Von Mises distribution.	8
2.3	Representation of the similarity between a Von Mises and wrapped normal distributions on the interval $[0, 2\pi]$	8
2.4	Wrapped Dirac Distribution.	9
3.1	Bessel ratio $\frac{I_1(\kappa)}{I_0(\kappa)}$ plotted using the libDirectional toolbox.	24
4.1	Uniform linear array representation (extracted from [1]).	29
4.2	Direction of Arrival model considered (extracted from [1]).	30
4.3	Arduino Nano connected to external memory.	32
4.4	Arduino Nano and external memory connection circuit.	32
4.5	Omnidirectional Microphone and its pre amplification circuit.	32
5.1	Representation of the geometrical strategy to obtain the pedestrian position at time k	35
5.2	Simple diagram is presented for the linear Kalman filter operation in the constant velocity model.	38
6.1	Wrapped Normal approximations for measured angles 30° , -30° , 0° and 40°	40
6.2	Three-dimensional representation of Wrapped Normal approximations for measured angles 30° , -30° , 0° and 40°	40
6.3	Room with dimensions 7×7 and positioned sensors.	42
6.4	Measurements for sensor 1 at (1,1.15) and sensor 2 at (1,1).	42
6.5	Measurements for sensor 1 at (3,1.15) and sensor 2 at (3,1).	43
6.6	Measurements for sensor 1 at (2,3) and sensor 2 at (2,1).	43
6.7	Measurements for sensor 1 at (2,5) and sensor 2 at (2,1).	44
6.8	Dirac components for two measured angles.	44
6.9	State estimation of the pedestrian position with fixed R, linear Kalman filter and Constant Velocity model.	45
6.10	State estimation of the pedestrian position with varying R, linear Kalman filter and Constant Velocity model.	45

6.11 State estimation of the pedestrian position with linear Kalman filter and Lavegin model.	46
6.12 State estimation of the pedestrian position with EKF and Lavegin model.	47
6.13 State estimation of the pedestrian position with EKF and Constant Velocity model. .	48
6.14 State estimation of the pedestrian position with UKF and Lavegin model.	48
6.15 State estimation of the pedestrian position with UKF and Constant Velocity model. .	49

List of Tables

6.1	Comparison of the WN parameters obtained for different angles.....	39
6.2	Comparison of the RMSEs obtained for the different filter approaches considering the constant velocity model.	50
6.3	Comparison of the RMSEs obtained for the different filter approaches considering the Lavegin model.	50

List of symbols

Greek symbols

μ	Parâmetro estatístico
σ	Parâmetro estatístico
Δ	Varição entre duas grandezas similares
κ	Parâmetro estatístico

Superscripts

\cdot	Varição temporal
$-$	Valor médio
$\hat{}$	Valor estimado

Acronyms

ABNT	Associação Brasileira de Normas Técnicas
WN	Wrapped Normal
VM	Von Mises
WD	Wrapped Dirac Mixtures
MATLAB	Marca registrada da MathWorks, Inc.
DOA	Direction of arrival
TDOA	Time difference of arrival
A/D	Analógico para digital
SPI	Serial Peripheral Interface

Chapter 1

Introduction

1.1 Motivation

For a long time now, humankind has developed techniques to deal with circular nature problems. The compass and the clock were extremely important tools for navigation, for instance. Where typical observations that are measured by the compass include directions of migrating birds and wind directions [2]. Therefore, not only providing a sense of orientation, but allowing studies for scientific fields such as biology or even geology (magnetic pole).

That aforementioned sense of orientation also arises in the ability of locating acoustic sources. For instance, when searching for a concert in a unknown area, the direction of higher noise or music patterns will act as guidelines. Inspired by this capacity of estimating a direction for the acoustic waves, sensors based on time difference of arrival (TDOA) have been presented on the literature [3], [4]. That way providing angular information that can be used on tracking experiments, for instance [5].

The problem of tracking based solely on angular measurements has been well developed and addressed on the literature [6], [7], [8]. Solutions based on nonlinear Kalman filters [9] or more elegant ones considering pseudomeasurements [10] have been presented to approach this kind of problem. However, most solutions fail to consider correctly the statistics of the measured angles, assumed to be associated to a gaussian distribution. A correct treatment to those angles must consider the mathematical background provided by directional statistics [11]. The filters proposed in [12], [5] and [13] consider circular distributions in order to improve their performances given highly uncertain measurements.

In [1] a low-budget sensor based in the time difference of arrival (TDOA) was presented and implemented. However, the sensor only provides static angular estimation, i.e., the acoustic source does not move while measurements are made. Therefore, the aim of this work is to evaluate the performance of traditional filtering algorithms (EKF and UKF) and a filter based on circular statistics, given measurements provided by the aforementioned sensor, for pedestrian indoor tracking. Hence, the goal of this work is to argue in favor of circular statistic considerations for angular measurements to improve pedestrian tracking in indoor environments. The analysis provided by

this work can easily be extended to other applications where angular measurements are considered.

1.2 Problem Statement

The position over time of a pedestrian walking in a room is an information of interest. Two low cost DOA sensors, each containing two omnidirectional microphones in a linear uniform array, are capable of estimating angular directions of an acoustic source and sending it to a processing unit (robot). The processing unit is embedded with a filtering algorithm capable of estimating the pedestrian position at each time step. The objective of the robot is to determine the pedestrian path considering the angular uncertainty of the measurements. In order to provide a reliable ground truth for the estimated positions, the chosen path considered aspects such as ease of implementation and evaluation. Therefore, the pedestrian route was assumed to be a straight line. Figure 1.1 provides a better visualization of the problem.

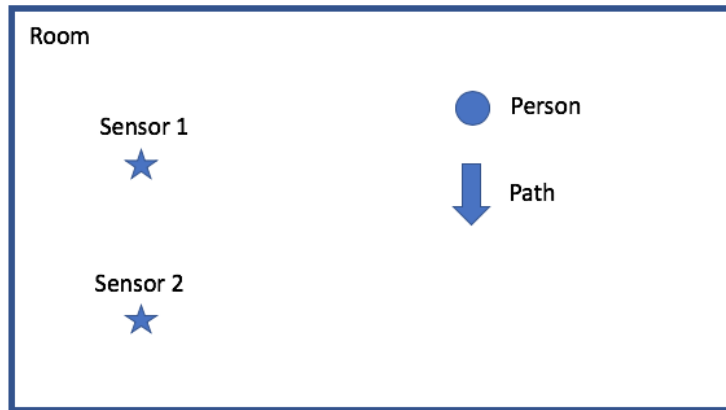


Figure 1.1: Visualization of the stated problem to be approached.

In [1], DOA sensors capable of estimating an acoustic source direction were developed and evaluated. As an extension of that work, since the sensors were only tested for fixed source directions, it is proposed a filtering approach to perform the tracking of a moving acoustic source. Since the sensors were motivated and developed considering the problem of detecting the orientation of a human whistle, the pedestrian is assumed to be whistling in a room, or emitting the whistle frequency artificially.

Since the sensor measurements are directions, their circular nature had to be considered. Therefore, an approach that made use of directional statistics to model and deal with the uncertainties in the measurements had to be fused with the filtering algorithm. In order to do so, traditional filtering algorithms and circular filtering algorithms had to be studied and evaluated. Since traditional solutions for bearings only measurements consider EKF or UKF [9], those filters were also implemented for comparison purposes.

To predict the future position of the pedestrian based on a current estimate, two slightly different constant velocity models were employed in the simulations. The first model was a Lavegin model, that seemed to portrait well the time-varying locations of a person in a room [14][15]. The

second model was a simpler one, considering that the pedestrian motion would be over a straight line, considering regular variations in position for each time step.

A series of simulations were performed taking into consideration the problems described herein in order to provide good filtering approximations for the pedestrian position. Different filters and models were simulated and compared so an evaluation for a real implementation could be made.

1.3 Outline

The following chapters are presented as follows:

Chapter 2 collects some basics on circular statistics [11], [2], defining the manifold and the problems when dealing with circular data. Initially, a new definition of mean is presented to consider the inherent problems of angular direction. Then, a definition for the circular probability distributions is given, describing some of their properties. Subsequently, the most relevant models to represent circular data are described with their respective characteristics. In the sequence, the definition of trigonometric moments is stated and some results for given distributions are presented. At last, the circular equivalent result for the central limit theory is mentioned.

Chapter 3 presents an introduction to estimation theory, in order to provide some mathematical background for the development of the filters. First, maximum likelihood and bayesian estimation methods are presented. In the sequence, a discussion about scalar and vector valued data for the development of the Kalman filter is made. Subsequently, linear and nonlinear Kalman filters are described and their algorithms are introduced. Finally, a circular filter based on moment matching was derived and their algorithms presented.

Chapter 4 presents the topic of DOA estimation, describing the low-budget sensors that will be considered and a brief discussion on implementation is given.

Chapter 5 introduces a discussion in measurement equations, developing conditions for a non traditional approach in pedestrian tracking. In addition, a model for pedestrian motion is presented.

In Chapter 6, a treatment is given for the sensor noisy measurements and results for simulations of different kinds of filters are presented. Besides, their performances are compared for numerous cases and implementation in real time estimation is evaluated.

At last, Chapter 7 provides remarks concerning the simulations, their results and limitations, proposing further developments for future works.

Chapter 2

Topics in Circular Statistics

This chapter aims to introduce some concepts of directional statistics that will be of great use in the development of the circular filter. First, we will start with the definition of the unit circle manifold and circular random variables. Then, some circular distributions of interest will be presented and properties will be derived. The content of the following subsections were inspired by the approach given in [16],[11] and [2].

2.1 The Unit Circle

Circular statistics is a specialization of a branch of statistics called Directional statistics, which studies angles or directions. The manifold our discussion will be focusing is the unit circle S^1 . A very intuitive and useful definition for S^1 would be $\{x \in \mathbb{C} : |x| = 1\}$, the subset of all complex numbers with unit norm. In order to construct a bijection, consider the mapping $l_1 : \mathbb{C} \mapsto [0, 2\pi)$ with

$$l_1 : x \mapsto \text{Arg}(x).$$

Where the $\text{Arg}(\cdot)$ function is the argument of a complex number and can be defined as

$$\text{Arg} : \mathbb{C} \setminus \{0\} \mapsto [0, 2\pi) , x \mapsto \text{atan2}(\text{Im}(x), \text{Re}(x)).$$

The atan2 function is the well known four-quadrant inverse tangent. This function is a necessary extension since the ordinary \arctan function is only defined in intervals of length π . The formal definition of $\text{atan2} : \mathbb{R}^2 \mapsto [0, 2\pi)$ is given bellow

$$\text{atan2}(y, x) = \begin{cases} \arctan(y/x), & x > 0, y \geq 0 \\ \arctan(y/x) + 2\pi, & x \geq 0, y < 0 \\ \pi/2, & x = 0, y > 0 \\ 3\pi/2, & x = 0, y < 0 \\ \text{undefined}, & x = 0, y = 0 \\ \arctan(y/x) + \pi, & x < 0 \end{cases}$$

The function l_1 has a natural inverse mapping:

$$l_1^{-1} : x \mapsto \cos(x) + i \sin(x)$$

Thus, exists a bijection between S^1 and $[0, 2\pi)$ and allow us to parametrize the circle as the interval $[0, 2\pi) \subset \mathbb{R}$. This definition is very appealing since S^1 with the topology induced by l_1 has addition and inversion as continuous functions. Moreover, addition on $[0, 2\pi)$ modulo 2π is comparable to multiplication in \mathbb{C}

$$\alpha + \beta = l_1(l_1^{-1}(\alpha) \times_{\mathbb{C}} l_1^{-1}(\beta)).$$

Where $\times_{\mathbb{C}}$ is complex multiplication in \mathbb{C} . More details are given in [16].

2.2 Circular Data

When dealing with circular data, it is of interest to characterize the data by its statistics such as mean and variance. However, the direct use of mean in a set of angular values might lead to wrong results in terms of the mean direction, since it depends on the choices of zero direction and sense of rotation [11]. To get a proper analysis, it is more interesting to work with transformations from polar coordinates to rectangular ones, i.e., given a set of n circular observations $\alpha_1, \dots, \alpha_n$, obtain their coordinates in terms of sines and cosines

$$(\cos(\alpha_i), \sin(\alpha_i)), \quad i = 1, \dots, n$$

The resultant vector of these n unit vectors is given by

$$\mathbf{R} = \left(\sum_{i=1}^n \cos \alpha_i, \sum_{i=1}^n \sin \alpha_i \right) = (C, S).$$

That way the length of the resultant vector is given by $R = \sqrt{C^2 + S^2}$ and the mean direction $\bar{\alpha}_0$ is given by

$$\bar{\alpha}_0 = \text{atan2}(S/C).$$

Now that a proper treatment for the mean direction was given, it's time to present some probability distributions for circular random variables.

2.3 Circular Probability Distributions

A circular distribution, to put it simply, is a probability distribution which all probability is allocated along the unit circle S^1 . Random variables with this kind of distribution are called circular random variables in literature [11], [2]. In order to characterize such distribution we should take a look at its distribution function $F(\cdot)$. Suppose an initial angle θ in S^1 is chosen. Then the distribution can be associated with that angle, and $F(\cdot)$ is defined as the function on the whole real line given by

$$F(x) = \Pr(0 < \theta \leq x), \quad 0 \leq x \leq 2\pi,$$

and

$$F(x + 2\pi) - F(x) = 1, \quad -\infty < x < \infty,$$

which states that the probability in any arc of length 2π on S^1 is equal to 1 [2].

Still according to [2], if the distribution F is absolutely continuous then it has a probability density function f which satisfies:

$$\int_{\alpha}^{\beta} f(\theta) d\theta = F(\beta) - F(\alpha), \quad -\infty < \alpha \leq \beta < \infty$$

In addition, f satisfies 3 basic properties:

1. $f(\theta) \geq 0$;
2. $\int_0^{2\pi} f(\theta) d\theta = 1$;
3. $f(\theta) = f(\theta + k \cdot 2\pi)$, for all $k \in \mathbb{Z}$, i.e, f is periodic.

2.3.1 Circular Models

In this section we aim to describe a few important distributions in S^1 . As presented so far, a circle random variable can be expressed in terms of an angle θ or as a two dimensional unit vector (X, Y) where $X = \cos(\theta)$ and $Y = \sin(\theta)$. Some of the notorious circular distributions arise from known probability distributions in \mathbb{R} or \mathbb{R}^2 . Therefore, a few general methods for generating such distributions are presented in [11], [2] and are worth mentioning, such as:

- (i) wrapping a distribution on the real line along the unit circle;
- (ii) Characterizing properties such as maximum entropy;
- (iii) Transforming a random variable in \mathbb{R}^2 to just its directional component, the so called *offset distributions*.

2.3.2 Wrapped Normal

Any random variable in \mathbb{R} can be transformed into a circular one by performing a reduction to module 2π operation, i.e., we define:

$$\theta = x(\bmod 2\pi). \tag{2.1}$$

Such an operation corresponds to wrapping the real line around the unit circle radius, accumulating overlapping points probabilities. Which means that for any $\theta \in [0, 2\pi)$ the probabilities of $\theta \pm 2\pi$, $\theta \pm 4\pi, \dots$ will be accumulated in θ . Therefore, a function that does such a mapping cannot be injective, since an angle $\theta \in S^1$ will have a great number of preimages in the real line. Consider that $g(y)$ is a probability density function (p.d.f.) in the real line, we can define a circular one $f(\theta)$ as it follows:

$$f(\theta) = \sum_{m=-\infty}^{\infty} g(\theta + 2\pi m), \quad 0 \leq \theta < 2\pi. \tag{2.2}$$

If the function $g(y) = \mathcal{N}(\mu, \sigma^2)$, we can apply it directly in the equation 2.2 to obtain the so called Wrapped Normal distribution.

$$f(\theta) = \frac{1}{\sigma\sqrt{2\pi}} \sum_{m=-\infty}^{\infty} \exp\left[\frac{-(\theta - \mu - 2\pi m)^2}{2\sigma^2}\right]. \quad (2.3)$$

A three-dimensional representation of this distribution can be observed in figure 2.1.

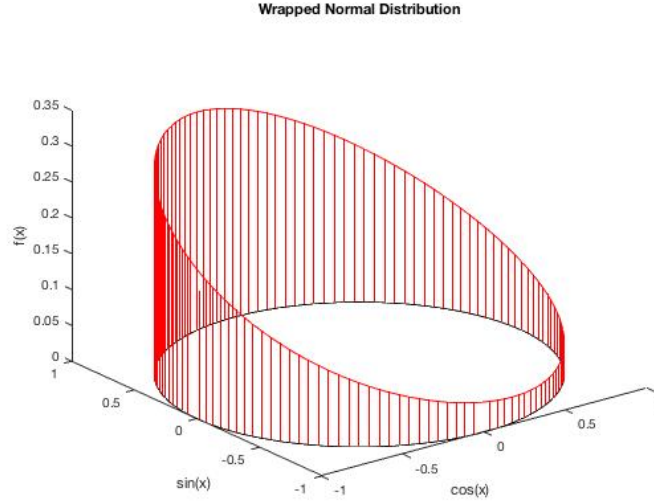


Figure 2.1: Three-dimensional representation of a wrapped normal distribution.

2.3.3 Von Mises or Circular Normal

The following distribution was first introduced as a statistical model by Von Mises in 1918 [11]. Also referred as circular normal, this distribution is characterized by its properties that resemble the Normal distribution on the real line. For that reason this distribution has been extensively studied and is the main model in applications involving circular data [17], [18], [19]. The Von Mises probability density function is given by:

$$f(\theta; \mu, \kappa) = \frac{1}{2\pi I_0(\kappa)} e^{\kappa \cos(\theta - \mu)}, \quad 0 \leq \theta < 2\pi, \quad (2.4)$$

where $\mu \in S^1$ and $\kappa > 0$ are the location parameter and concentration parameter, respectively. In the normalization constant, $I_0(\cdot)$ represents the modified Bessel function of order 0 and is defined as:

$$I_0(\kappa) = \frac{1}{2\pi} \int_0^{2\pi} \exp(\kappa \cos(\theta)) d\theta = \sum_{r=0}^{\infty} \left(\frac{\kappa}{2}\right)^{2r} \left(\frac{1}{r!}\right)^2. \quad (2.5)$$

The Von Mises distribution is obtained by restricting a two-dimensional Gaussian with mean $|\mu| = 1$ and covariance $\kappa \cdot \mathbf{I}_{2 \times 2}$, where $\mathbf{I}_{2 \times 2}$ is the identity matrix, to the unit circle and remapping

it to $[0, 2\pi)$. The main reason this distribution is so useful is that it is closed under bayesian inference, that will later be presented in the development of the filter [20].

A 3D representation of this distribution is shown in figure 2.2. The 2D representation of both mentioned distributions can be observed in the figure 2.3. It is important to notice the similarity between those curves. For figure 2.3 the parameter μ was set to π for both distributions, and parameters σ and κ were unitary.

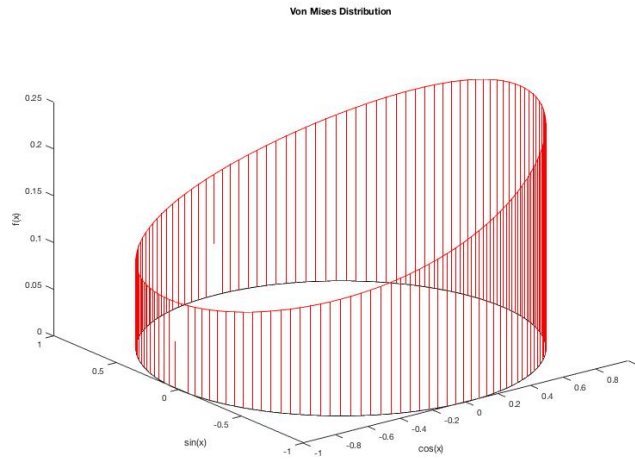


Figure 2.2: Three-dimensional representation of a Von Mises distribution.

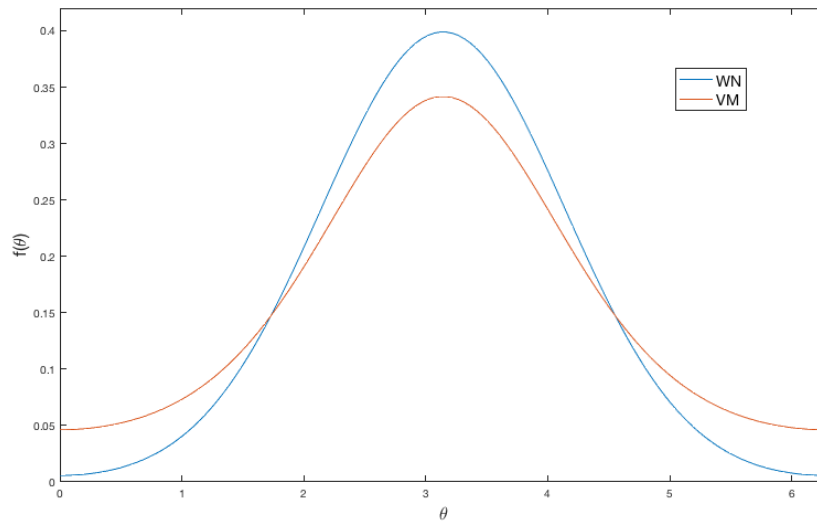


Figure 2.3: Representation of the similarity between a Von Mises and wrapped normal distributions on the interval $[0, 2\pi]$.

2.3.4 Wrapped Dirac Mixture

Another important distribution that needs to be given some attention is the wrapped Dirac mixture distribution. The definition of this distribution is very similar to a finite weighted impulse train in the real line. The only difference from the Dirac mixture to the one described is that the positions belong to S^1 . Therefore, we define the wrapped Dirac mixture (WD) with L components as:

$$f(x; \gamma_1, \dots, \gamma_L, \beta_1, \dots, \beta_L) = \sum_{j=1}^L \gamma_j \delta(x - \beta_j) \quad (2.6)$$

with Dirac delta distribution $\delta(\cdot)$, Dirac positions $\beta_1, \dots, \beta_L \in S^1$, and weights $\gamma_1, \dots, \gamma_L > 0$, where $\sum_{j=1}^L \gamma_j = 1$. A representation of the aforementioned distribution can be observed in figure 2.4.

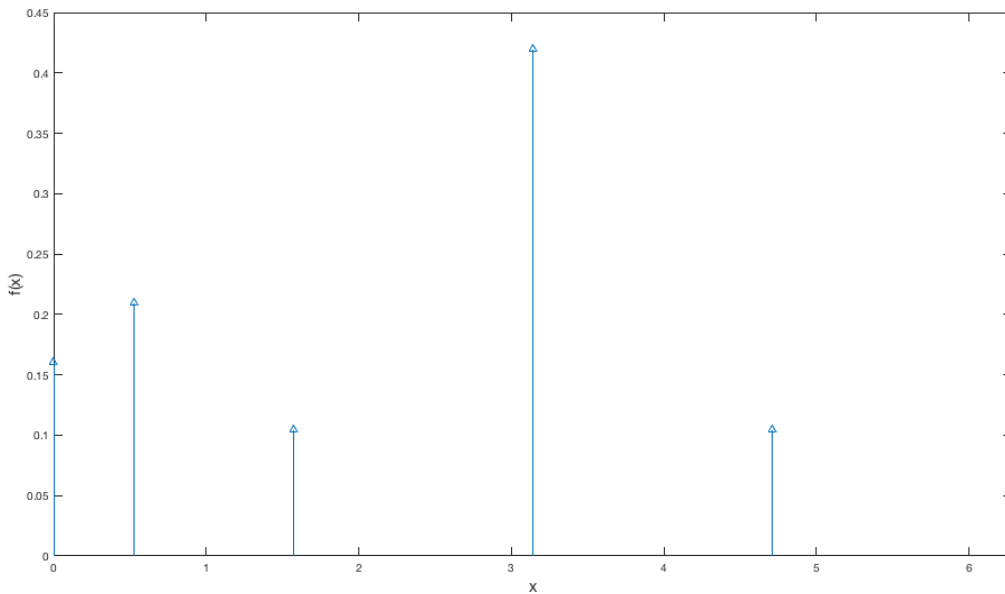


Figure 2.4: Wrapped Dirac Distribution.

The equation (2.6) emphasizes the discrete aspect of the WD. There is an interest in a discrete probability distribution in a continuous domain since it can be used for sampling a continuous distribution in a particular manner. That way, a discrete approximation for continuous distributions can be achieved which can be of use when facing non-linear systems.

2.4 Trigonometric Moments

Statistical moments always appear when dealing with estimation problems, since they provide a characterization of the probability distribution. The mean and variance of a distribution are respectively the first and second statistical moments and are indicators of the location and concentration (towards its mean) of a distribution. When dealing with circular statistics there also

exist moments, they are called trigonometric or circular moments.

For a random variable $x \sim f(x)$ defined on S^1 , we define the n -th trigonometric moment of x by:

$$\begin{aligned} m_n &= \mathbb{E}\{\exp(ix)^n\} = \mathbb{E}\{\exp(inx)\} \\ &= \int_0^{2\pi} \exp(inx)f(x)dx \end{aligned} \quad (2.7)$$

with i as the imaginary unit.

When dealing with distributions on the line, we characterize them by their mean and variance (which are the first and second moments). However, equation (2.7) points to the fact that m_n is a complex number, therefore having a real and an imaginary part. Due to having two degrees of freedom, parameters that are equivalent to both those characterizing ones can be obtained from the first trigonometric moment [11], [2]. The circular mean is defined as $\arg m_1 = \text{atan2}(\text{Im}(m_1), \text{Re}(m_1))$, and the concentration (sometimes called circular variance) as $|m_1| = \sqrt{(\text{Re}(m_1))^2 + (\text{Im}(m_1))^2}$. In addition, the VM and WN distributions are uniquely defined by their first trigonometric moments as presented in [2].

The trigonometric moments of the distributions presented so far are:

$$m_n^{WN} = \exp(in\mu - \frac{n^2\sigma^2}{2}); \quad (2.8)$$

$$m_n^{VM} = \exp(in\mu) \frac{I_{|n|}(\kappa)}{I_0(\kappa)}; \quad (2.9)$$

$$m_n^{WD} = \sum_{j=1}^L \gamma_j \exp(in\beta_j). \quad (2.10)$$

Proofs can be found in [11], [2]. The term $I_n(\cdot)$ in equation 2.9 is the modified Bessel function of order n [21]. The quotient of Bessel functions should be calculated numerically with the algorithm by [22].

2.5 Circular Central Limit Theorem

2.5.1 Central Limit Theorem

When studying probability and statistics on the real line or when dealing with random variables in engineering problems (communications, information theory), the central limit theorem (CLT) presents itself as very recurrent and useful result. Suppose a sequence of independent and identically distributed (i.i.d.) random variables X_i are drawn from a distribution of mean μ and (finite) variance σ^2 . The average sum of the terms of the sequence is given by:

$$A_n := \frac{X_1 + \dots + X_n}{n}.$$

The law of large numbers states that A_n converges to μ when $n \rightarrow \infty$ [23]. As n gets larger, the distribution of the difference between the sample average S_n and its limit μ - when multiplied by

the factor \sqrt{n} - approximates a normal distribution with zero mean and variance σ^2 . The central limit theorem then states that as n approaches infinity:

$$\sqrt{n}(A_n - \mu) \longrightarrow \mathcal{N}(0, \sigma^2),$$

or, in terms of the sum of the terms of the sequence:

$$\frac{nA_n}{\sqrt{n}} - \mu\sqrt{n} \longrightarrow \mathcal{N}(0, \sigma^2). \quad (2.11)$$

2.5.2 Circular equivalent

It's not surprising that such a result has an equivalent to the circular data case. Suppose now that $(\alpha_1, \dots, \alpha_n)$ is an i.i.d. sample from a common (non-lattice) circular distribution with cumulative distribution function (cdf) $G(\theta)$. Then the distribution of the sum

$$S_n = (\alpha_1 + \dots + \alpha_n) \pmod{2\pi}$$

converges to the uniform distribution on the circle as n approaches infinity, as presented in [11], [2]. For convenience, assume that the α_i 's are on the interval $(-\pi, \pi)$ with $E(\alpha_i) = 0$ and $E(\alpha_i^2) = \sigma^2$. By equation 2.11:

$$\frac{\sum_{i=1}^n \alpha_i}{\sqrt{n}} \longrightarrow \mathcal{N}(0, \sigma^2)$$

as $n \rightarrow \infty$. That way, by performing a modulo 2π operation it yields the circular equivalent to the CLT:

$$S_{n*} := \frac{\sum_{i=1}^n \alpha_i}{\sqrt{n}} \pmod{2\pi} \longrightarrow WN(0, \sigma^2) \quad (2.12)$$

as $n \rightarrow \infty$.

Chapter 3

Topics in Estimation and Filtering Algorithms

In the previous chapter we discussed about a field of directional statistics that focus on the unit circle. Some distributions on that manifold were presented as well as some interesting properties. This chapter aims to provide some basis on estimation theory and the theoretical development of a suitable filter for position estimation in tracking problems with angular measurements.

3.1 Estimation Theory

3.1.1 Maximum Likelihood

The aim of statistical inference, to put it simply, is to make certain determinations with regard to the unknown parameters figuring in the underlying distribution. In practical terms what we want to do is to construct an estimator for θ , that is, a known function $\hat{\theta}$ of the the random sample X_1, \dots, X_n [24]. Clearly, if x_1, x_2, \dots, x_n are the observed values of the random sample, then the observed value of our estimate will be $\hat{\theta}(x_1, \dots, x_n)$. One of the most accepted principle for constructing this estimator is the maximum likelihood (ML).

The likelihood function is defined as

$$L(\theta|x_1, \dots, x_n) = \prod_{i=1}^n f(x_i|\theta)$$

and represents a joint p.d.f. of the x_i 's, for the observed values of the X_i 's as a function of θ . The maximum likelihood principle consists in maximizing the likelihood function with respect to θ . The maximizing point (assuming it exists and is unique) is a function of x_1, \dots, x_n , and is what we call the Maximum Likelihood Estimate (MLE) of θ , as presented in [24], [23]. The common notation used for the likelihood function is $L(\theta|x_1, \dots, x_n)$ and for the log-likelihood is $l(\theta|x_1, \dots, x_n)$. The θ parameter can be a vector which we would like to estimate the mean and variance, or μ and σ parameters for a WN distribution, for instance.

3.1.2 Bayesian Estimation

In this section, a brief discussion is presented of still another approach to parameter estimation, which, unlike the previous approach, is kind of penalty driven [24]. For the bayesian paradigm, θ is considered to be a random variable with a given prior distribution $f_\theta(\theta)$. Consider, like in the discussion of the likelihood function, that a vector of samples or measurements $\mathbf{x} = X_1, \dots, X_n$ of θ is taken. Therefore, by the Bayes rule it yields that

$$f(\theta|\mathbf{x}) = \frac{f(\mathbf{x}|\theta)f_\theta(\theta)}{f_\mathbf{x}(\mathbf{x})} = \frac{f(\mathbf{x}|\theta)f_\theta(\theta)}{\int_{-\infty}^{\infty} f_\mathbf{x}(\theta)f_\theta(\theta)d\theta}.$$

By the definition introduced in the previous section, it is clear that the term $f(\mathbf{x}|\theta)$ is a likelihood function. The term $f(\theta|\mathbf{x})$ is called posteriori density and represents the p.d.f. of θ for given measurements. Assuming that $f_\mathbf{x}(\mathbf{x})$ and θ are independent, we can rewrite the previous equation as:

$$f(\theta|\mathbf{x}) = cf(\mathbf{x}|\theta)f_\theta(\theta),$$

where $c = \frac{1}{f_\mathbf{x}(\mathbf{x})}$. In addition, With the assumption that all the components x from \mathbf{x} are independent than $f(\mathbf{x}|\theta) = \prod_{k=1}^n f(x_k|\theta)$, which can ease the process of computing $f(\theta|\mathbf{x})$.

In this kind of approach the bayesian estimate $\hat{\theta}$ can be given in different manners, being the most common the use of the mean as the estimate. That implies that the estimate $\hat{\theta}$ is given by

$$\hat{\theta} = \mathbb{E}(\theta|\mathbf{x}) = \int_{-\infty}^{\infty} \theta f(\theta|\mathbf{x})d\theta,$$

as referred in [23] and detailed in [24].

3.2 Filtering Algorithms

Aside from the methods presented in the previous section, there are other techniques that can be applied to approach a solution for parameters or state estimations. In fact, when dealing with linear estimation problems, Kalman filter based approaches are a far more common in recent literature than bayesian ones.

3.2.1 Prerequisites

In [25] a discussion about scalar and vector-valued data is presented in order to provide the mathematical background necessary to the development of the traditional Kalman filter. There, an optimal estimator in the least mean squares (l.m.s.) sense is developed in order to minimize the cost function $E\{(x - \hat{x})^2\}$, where x is a random variable or vector and \hat{x} its estimate.

For an unobservable variable x given a measurement y , the estimator is a function of the measurement $\hat{x} = h(y)$. That works for x and y be either scalar or vector-valued and the problem

consists on minimizing the cost function:

$$\min_{h(\cdot)} \mathbb{E}\{x - \hat{x}\}^2.$$

The solution for the scalar case given in [25] to this problem is

$$\hat{x} = h(y) = \mathbb{E}\{x|y\},$$

with minimum cost $\mathbb{E}\{x - \hat{x}\}^2 = \sigma_x^2 - \sigma_y^2$ since it's unbiased. Thus, for vector-valued data when x and y are vectors:

$$\begin{bmatrix} \hat{x}(0) \\ \hat{x}(1) \\ \dots \\ \hat{x}(m-1) \end{bmatrix} = \begin{bmatrix} h_0(y(0), y(1), \dots, y(n-1)) \\ h_1(y(0), y(1), \dots, y(n-1)) \\ \dots \\ h_{m-1}(y(0), y(1), \dots, y(n-1)) \end{bmatrix}.$$

The problem consists in minimizing each component of x , which can be represented as

$$\min_{\{h_k(\cdot)\}} \mathbb{E}\{\tilde{x}^* \tilde{x}\} \quad \text{and} \quad \min_{\{h_k(\cdot)\}} \text{Tr}(R_{\tilde{x}})$$

where $\tilde{x} = x - \hat{x}$ and $R_{\tilde{x}} := \mathbb{E}\{\tilde{x}^* \tilde{x}\}$ is the covariance matrix of \tilde{x} . The solution given in [25] is:

$$\hat{x} = \mathbb{E}\{x|y\} := \begin{bmatrix} \mathbb{E}\{x(0)|y\} \\ \mathbb{E}\{x(1)|y\} \\ \dots \\ \mathbb{E}\{x(m-1)|y\} \end{bmatrix}.$$

Even though that discussion about random variables and vectors may have given an closed optimal solution for the estimation problem, it is not usually an easy task to find the conditional probability between them. For that reason, a whole chapter about linear estimation is presented in [25] to give a complete basis for the development of the Kalman filter. When considering linear estimation, a restriction is implicit upon \hat{x} which is

$$\hat{x} = h(y) = Ky + b$$

where K is a $m \times n$ matrix and b is a $m \times 1$ vector.

Derivations are made assuming that x and y are zero-mean random variables and the optimal linear l.m.s. estimator is presented

$$\hat{x} = K_o y,$$

where K_o represents any solution of the normal equations $K_o R_y = R_{xy}$ with R_y and R_{xy} being covariance matrices.

In the measurement of the state x , the r.v.'s x and y are related through the following linear model:

$$y = Hx + v,$$

where v is a random noise vector with covariance matrix R_v . It is assumed in [25] that the covariance of x is known, that x and v are uncorrelated (as we would expect), and the matrices R_x and R_v are positive definite.

It is shown, by the positive definite assumption, that the solution K_0 is unique for normal equations and the estimator is given by

$$K_0 = R_{xy}R_y^{-1} \rightarrow \hat{x} = R_{xy}R_y^{-1}y.$$

Also, the covariance matrices can be expressed in terms of the matrices H, R_x and R_v

$$R_y = \mathbb{E}\{yy^*\} = \mathbb{E}\{(Hx + v)(Hx + v)^*\} = HR_xH^* + R_v, \text{ since } \mathbb{E}\{xv^*\} = 0.$$

Then another expression for \hat{x} can be derived

$$\hat{x} = R_{xy}R_y^{-1}y = R_xH^*[R_v + HR_xH^*]^{-1}y,$$

and the resulting minimum square error for the estimate is

$$R_{\hat{x}} = [R_x^{-1} + H^*R_v^{-1}H]^{-1}.$$

3.2.2 Kalman Filter

To motivate the discussion about the Kalman filter, let's consider the following state-space model:

$$x_{k+1} = F_kx_k + G_kn_k, k \geq 0, \quad (3.1)$$

where x_k is the state-vector, n_k is the noise of the process and F_k and G_k are matrices that describe the evolution of x_k according to the previous value and the noise respectively. In addition, consider the same measurement model presented for linear estimation approaches, i.e.,

$$y_k = H_kx_k + v_k, k \geq 0 \quad (3.2)$$

with measurement noise v_k .

In [25] it is assumed that v_k and n_k are zero-mean white noises and have covariances and cross-covariances as presented below:

$$\mathbb{E} \begin{bmatrix} n_k \\ v_k \end{bmatrix} \begin{bmatrix} n_k \\ v_k \end{bmatrix}^* = \begin{bmatrix} Q_k & S_k \\ S_k^* & R_k \end{bmatrix} \delta_{ij},$$

where δ indicates the Kronecker delta. Also, the initial state x_0 is assumed to have zero mean, covariance Π_0 and to be uncorrelated to the process and measurement noises.

The key for performing Kalman filtering is its innovations process. It is shown in [25] that the problem of estimating x given y is equivalent to estimating x given $e = Ay$. Also, due to orthogonality principles of l.m.s. estimations, it is derived an expression for each e_k , that is

$$e_k := y_k - \hat{y}_{k|k-1}. \quad (3.3)$$

Thus, the estimator itself can be written as

$$\hat{x}_{|N} = \hat{x}_{|N-1} + (\mathbb{E}\{xe_N^*\})R_{e,N}^{-1}e_N. \quad (3.4)$$

Therefore, the innovations process for the system described in equation 3.1 will be

$$e_k = y_k - \hat{y}_{k|k-1} = y_k - H_k \hat{x}_{k|k-1} ,$$

$$\hat{x}_{k|k-1} = F_k \hat{x}_{k-1} + K_{p,k} e_k ,$$

where $K_{p,k} := (\mathbb{E}\{x_{k+1}e_k^*\})R_{e,k}^{-1}$ and $R_{e,k} := \mathbb{E}\{e_k e_k^*\}$ for $k \geq 0$ with $\hat{x}_{0|-1} = \mathbb{E}\{x_0\} = 0$. The state covariance matrix is defined as

$$\Pi_k := \mathbb{E}\{x_k x_k^*\}.$$

Following from the state-space model that the evolution of Π_k over time is

$$\Pi_{k+1} = F_k \Pi_k F_k^* + G_k Q_k G_k^*.$$

In a similar way, it can be derived a recursive formula for the covariance matrix $\Sigma_k := \mathbb{E}\hat{x}_{k|k-1}\hat{x}_{k|k-1}^*$ as it follows:

$$\Sigma_{k+1} = F_k \Sigma_k F_k^* + K_{p,k} R_{e,k} K_{p,k}^* ,$$

with $\Sigma_0 = 0$. By defining $P_{k|k-1} := \mathbb{E}\{\tilde{x}_{k|k-1}\tilde{x}_{k|k-1}^*\}$, it is demonstrated through orthogonality arguments that the state covariance can be expressed as

$$P_{k+1|k} = \Pi_{k+1} - \Sigma_{k+1} ,$$

which yields the famous **Riccati recursion**:

$$P_{k+1|k} = F_k P_{k|k-1} F_k^* + G_k Q_k G_k^* - K_{p,k} R_{e,k} K_{p,k}^* . \quad (3.5)$$

Since the cases that will be further approached consider that the process and measurement noises are uncorrelated, we have:

$$\mathbb{E} \begin{bmatrix} n_k \\ v_k \end{bmatrix} \begin{bmatrix} n_j \\ v_j \end{bmatrix}^* = \begin{bmatrix} Q_k & 0 \\ 0 & R_k \end{bmatrix} \delta_{ij} .$$

Where $\mathbb{E}\{n_k v_j^*\} = 0 \rightarrow S_k = 0$. And so the Kalman filter algorithm will be the following:

Algorithm 1: Kalman Filter (Measurement-Time Update Form, $S_k = 0$)

Start with $\hat{x}_{0|-1} = \mathbb{E}x_0$, $P_{0|-1} = \Pi_0$, R_0 , H_0 , y_0 , F_0 and at every time instant $k \geq 0$ compute:

1) Measurement Update:

$$\begin{aligned} R_{e,k} &= R_k + H_k P_{k|k-1} H_k^* \\ K_{f,k} &= P_{k|k-1} H_k^* R_{e,k}^{-1} \\ e_k &= y_k - H_k \hat{x}_{k|k-1} \\ \hat{x}_{k|k} &= \hat{x}_{k|k-1} + K_{f,k} e_k \\ P_{k|k} &= P_{k|k-1} - K_{f,k} H_k P_{k|k-1} \end{aligned}$$

2) Time update:

$$\begin{aligned} \hat{x}_{k+1|k} &= F_k \hat{x}_{k|k} \\ P_{k+1|k} &= F_k P_{k|k} F_k^* + G_k Q_k G_k^* \end{aligned}$$

3.2.3 Nonlinear Filtering

The Kalman filter previously presented is the most usual approach when dealing with linear systems. However, in various cases the measurement equations or the model (or both) are nonlinear which makes Kalman filter algorithms not a direct solution. For that reason, a number of different filtering techniques were presented over the years to approach these kind of situations [9], [14]. Among those different new methods, there are two Kalman based that deserves some special attention.

3.2.3.1 Extended Kalman Filter

This first method approaches the nonlinearities by a Taylor's series method. The key idea consists in making a first order approximation of the nonlinear functions in order to match the Kalman filter requirements and then apply its algorithm. To illustrate this, consider the following model and measurement equation (both nonlinear):

$$\begin{aligned} x_{k+1} &= f(x_k) + n_k, \quad k \geq 0 \\ y_k &= h(x_k) + v_k, \quad k \geq 0. \end{aligned} \tag{3.6}$$

In addition, we assume that the model and measurement noise processes are uncorrelated and zero-mean the same way presented for the Kalman filter.

If x is a scalar variable, the Taylor's series approximation around a point x_0 of $f(x)$ is given by

$$f(x) \sim \sum_{n=0}^{\infty} \frac{f^{(n)}(x_0)}{n!} (x - x_0)^n,$$

and its first order approximation is

$$f(x) \approx f(x_0) + f'(x_0)(x - x_0).$$

For the vector-valued case the result is similar, but instead of $f'(x_0)$ we have $\bar{F}(x_0)$ which is the Jacobian matrix of $f(x)$ with respect to the random variables contained in the vector x . Then the first order approximation around a point x_0 of the space-state model given in equation (3.6) is

$$\begin{aligned} x_{k+1} &\approx f(x_0) + \bar{F}(x_0)(x - x_0) + n_k \\ y_k &\approx h(x_0) + \bar{H}(x_0)(x - x_0) + v_k, \end{aligned}$$

where

$$\bar{F}(x_0) = \left. \frac{\partial f(x)}{\partial x} \right|_{x=x_0} \quad \text{and} \quad \bar{H}(x_0) = \left. \frac{\partial h(x)}{\partial x} \right|_{x=x_0}.$$

In order to achieve an expression that resembles more the Kalman filter model and measurement equations, we can introduce the following new variables:

$$\begin{aligned} \bar{y}_k(x_0) &= y_k - h(x_0) + \bar{H}(x_0)x_0 \\ \bar{u}(x_0) &= f(x_0) - \bar{F}(x_0)x_0. \end{aligned}$$

Then, the linearized state space model is given by:

$$\begin{aligned} x_{k+1} &\approx \bar{F}(x_0)x_k + n_k + \bar{u} \\ \bar{y}_k(x_0) &\approx \bar{H}(x_0)x_k + v_k, \end{aligned} \tag{3.7}$$

and the algorithm for the linearized equations is presented bellow.

**Algorithm 2: Extended Kalman Filter (Measurement-Time Update Form,
 $S_k = 0$)**

Start with $\hat{x}_{0|-1} = Ex_0$, $P_{0|-1} = \Pi_0$, and at every time instant $k \geq 0$ compute:

1) Measurement Update:

$$\begin{aligned}\hat{H}_k &= \bar{H}(\hat{x}_{k|k-1}) \\ R_{e,k} &= R_k + \hat{H}_k P_{k|k-1} \hat{H}_k^* \\ K_{f,k} &= P_{k|k-1} \hat{H}_k^* R_{e,k}^{-1} \\ e_k &= y_k - \hat{H}_k \hat{x}_{k|k-1} \\ \hat{x}_{k|k} &= \hat{x}_{k|k-1} + K_{f,k} e_k \\ P_{k|k} &= P_{k|k-1} - K_{f,k} \hat{H}_k P_{k|k-1}\end{aligned}$$

2) Time update:

$$\begin{aligned}\hat{F}_k &= \bar{F}(\hat{x}_{k|k-1}) \\ \hat{x}_{k+1|k} &= f(\hat{x}_{k|k}) \\ P_{k+1|k} &= \hat{F}_k P_{k|k} \hat{F}_k^* + Q_k\end{aligned}$$

3.2.3.2 Unscented Kalman Filter

The previously presented method (EKF) has a few problems with its implementation in various cases. Problems such as instability when timestep is not sufficiently small, or the complexity on computing the Jacobian matrices made necessary a search for a new method [14]. This second method introduces the use of the Unscented Transform, which is a deterministic sampling technique that estimates the statistics of a variable that undergoes nonlinear transformation. That way, the mean and covariance can be approximated and a Kalman filter approach is possible.

The key idea is to choose deterministically a set of points, called sigma points, in a way that they have the same mean and covariance as the original distribution. That way, each sigma point can be propagated through the nonlinear functions and a empirical mean and covariance can be calculated. This process avoids the need for Jacobian calculations and can be applied in a broader scope of systems. Consider that x is a n dimensional r.v. with mean \bar{x} and covariance P_{xx} . In [14] it is shown that the statistics of that variable can be encoded by $2n - 1$ weighted sigma points given by:

$$\begin{aligned}\mathcal{X}_0 &= \bar{x} & W_0 &= \kappa / (n + \kappa) \\ \mathcal{X}_i &= \bar{x} + (\sqrt{(n + \kappa) P_{xx}})_i & W_i &= 1 / (n + \kappa) \\ \mathcal{X}_{i+n} &= \bar{x} - (\sqrt{(n + \kappa) P_{xx}})_i & W_{i+n} &= 1 / (n + \kappa),\end{aligned}$$

where $i = 0, 1, \dots, n$, $\kappa \in \mathbb{R}$, $(\sqrt{(n + \kappa)P_{xx}})_i$ is the i th row or column of the matrix square root of $(n + \kappa)P_{xx}$ and W_i is the weight related to the i th sigma point. So an Unscented transformation can be summarized by the following steps:

Step 1: Apply the nonlinear transformation $f(x)$ to each sigma point \mathcal{X}_i in order to generate the set of transformed sigma points

$$\mathcal{Y}_i = f(\mathcal{X}_i).$$

Step 2: The mean of the transformed points is given by

$$\bar{y} = \sum_{i=0}^{2n} W_i \mathcal{Y}_i.$$

Step 3: Compute the covariance of the transformed points

$$P_{yy} = \sum_{i=0}^{2n} W_i (\mathcal{Y}_i - \bar{y})(\mathcal{Y}_i - \bar{y})^T.$$

That way an algorithm for the Unscented Kalman filter (UKF) can be derived, since the use of the Unscented Transform can predict the observation and innovation covariance and the cross covariance between the measurement and the state estimate. Also, it can be used to predict the state and its associated covariance. The algorithm for Unscented filtering for a model such as 3.6 is presented below.

Algorithm 3: Unscented Kalman Filter (Measurement-Time Update Form)

Start with $\hat{x}_{0|-1} = Ex_0$, $P_{0|-1} = \Pi_0$, and at every time instant $k \geq 0$ compute:

1) Measurement Update:

- Calculate the sigma points $\mathcal{X}_{i,k|k-1}$ around the predicted state $\hat{x}_{k|k-1}$
- Propagate the sigma points $\mathcal{X}_{i,k|k-1}$ through the observation model

$$\mathcal{Y}_{i,k|k-1} = h(\mathcal{X}_{i,k|k-1})$$

- Predict observation

$$\hat{y}_{k|k-1} = \sum_{i=0}^{2n} W_i \mathcal{Y}_{i,k|k-1}$$

- Compute the innovation covariance and cross covariance

$$P_{\tilde{y}\tilde{y}} = \sum_{i=0}^{2n} W_i (\mathcal{Y}_{i,k|k-1} - \hat{y}_{k|k-1})(\mathcal{Y}_{i,k|k-1} - \hat{y}_{k|k-1})^T + R$$

$$P_{x\tilde{y}} = \sum_{i=0}^{2n} W_i (\mathcal{X}_{i,k|k-1} - \hat{x}_{k|k-1})(\mathcal{Y}_{i,k|k-1} - \hat{y}_{k|k-1})^T$$

- Estimate the state and its covariance matrix

$$K = P_{x\tilde{y}} P_{\tilde{y}\tilde{y}}^{-1}$$
$$\hat{x}_{k|k} = \hat{x}_{k|k-1} + K(y_k - \hat{y}_{k|k-1})$$
$$P_{k|k} = P_{k|k-1} - K P_{\tilde{y}\tilde{y}} K^T$$

2) Time update:

- Calculate the sigma points $\mathcal{X}_{i,k|k}$ around the estimate state $\hat{x}_{k|k}$
- Propagate the sigma points $\mathcal{X}_{i,k|k}$ through the process dynamics model

$$\mathcal{X}_{i,k+1|k} = f(\mathcal{X}_{i,k|k})$$

- Predict the next state

$$\hat{x}_{k+1|k} = \sum_{i=0}^{2n} W_i \mathcal{X}_{i,k+1|k}$$

- Predict the covariance

$$P_{k+1|k} = \sum_{i=0}^{2n} W_i (\mathcal{X}_{i,k+1|k} - \hat{x}_{k+1|k})(\mathcal{X}_{i,k+1|k} - \hat{x}_{k+1|k})^T + Q$$

3.2.4 Circular Filtering

Now the problem of estimation is extended to the circular case. A lot of different methods have been proposed to treat circular random variables [26], [27]. Traditional filters such as the Kalman Filter, EKF and UKF are unable to handle directional quantities explicitly, since they assume that a representation in \mathbb{R}^n is enough for state and measurements. However, such a representation leads to poor approximations, since they don't consider the inherent periodicity of those variables. Often, those approximations have a strong dependency with the quality of the initial estimate and fail the discontinuity between 0 and 2π is reached.

To avoid those kind of inconsistencies, directional statistics presents itself as a powerful tool. In chapter 2 an introduction to circular statistics has been made. There we described how to treat statistics for circular r.v.'s and some probability distributions were presented. An interesting approach for the circular filtering problem is given by [16] where moment matching techniques are applied to face nonlinear estimation.

Moment Matching This technique consists in approximating a circular distribution by another circular distribution in a way that eases the process of filtering and parameter estimations. The WD distribution is a discrete one, which makes it easier to propagate through nonlinear functions. That way, the authors in [28] present a way of approximating the WN and VM distributions by a number of Dirac components. This method resembles a lot the Unscented Transform previously presented for real line distributions. The trigonometric moments for the WN, VM and WD were presented in chapter 2 and are given by

$$\begin{aligned} m_n^{WN} &= \exp(in\mu - \frac{n^2\sigma^2}{2}); \\ m_n^{VM} &= \exp(in\mu) \frac{I_{|n|}(\kappa)}{I_0(\kappa)}; \\ m_n^{WD} &= \sum_{j=1}^L \gamma_j \exp(in\beta_j). \end{aligned}$$

Both the VM and WN distributions are uniquely defined by their first trigonometric moment, then positioning WD components to match it already gives a good approximation. In [26] derivations using $L = 3$ Dirac components are made and the WD distribution that matches a WN with parameters μ and σ is given by:

$$f^d(x) = \frac{1}{3}\delta(x - (\mu - \alpha)) + \frac{1}{3}\delta(x - (\mu)) + \frac{1}{3}\delta(x - (\mu + \alpha)),$$

where α is obtained by matching m_1^{WN} and $m_1^{f^d}$ and is equal to

$$\alpha = \arccos\left(\frac{3}{2} \exp(-\frac{\sigma^2}{2}) - \frac{1}{2}\right). \quad (3.8)$$

For the VM distribution the same procedure holds and its WD approximation is given by:

$$f^d(x) = \frac{1}{3}\delta(x - (\mu - \alpha)) + \frac{1}{3}\delta(x - (\mu)) + \frac{1}{3}\delta(x - (\mu + \alpha)),$$

where

$$\alpha = \arccos\left(\frac{3}{2} \frac{I_1(\kappa)}{I_0(\kappa)} - \frac{1}{2}\right). \quad (3.9)$$

When given a WD distribution, it is important to perform the reverse process and obtain the equivalent WN or VM p.d.f.. In both cases, the parameter μ is obtained by performing the following operation

$$\mu = \text{atan2}\left(\sum_{j=1}^L \sin(\beta_j), \sum_{j=1}^L \cos(\beta_j)\right). \quad (3.10)$$

Now for the σ parameter in the WN and the κ parameter in the VM, they are obtained by matching (once again) their first trigonometric moments:

$$\begin{aligned} \sigma &= \sqrt{-2 \log\left(\sum_{j=1}^L \omega_j \exp(i(\beta_j - \mu))\right)}, \\ \frac{I_1(\kappa)}{I_0(\kappa)} &= \exp(-i\mu) \sum_{j=1}^L L \omega_j \exp(i\beta_j). \end{aligned} \quad (3.11)$$

The parameter κ , as it can be observed in the expression above, needs to be calculated numerically. Since the Bessel ratio $\frac{I_1(\kappa)}{I_0(\kappa)}$ is always in the interval $[0, 1]$ as shown in figure 3.1 this function is not difficult to invert numerically [26]. An algorithm to compute the ratio of Bessel functions is given in [22].

Approaches with a higher number of Dirac components are presented in [28] and conditions for the choice of parameters are established. The moment matching technique, however, does not only consist in matches by Dirac mixtures. One can perform moment matching directly between a WN and VM distributions, for example. An algorithm to compute WN approximations of VM distributions or vice-versa is given in [26]. There, the loss of information in the approximations is presented in terms of Kullback-Leibler divergence [26] which validates moment matching results.

Filtering

On the previous sections a few filtering algorithms were presented in order to estimate space state variables. It is clear by now that two stages are necessary when filtering: prediction and measurement update. In the prediction stage the goal is to predict the distribution of the state in the next time step based on the system function, the estimated distribution of the current state and the distribution of the system noise. Nevertheless, the measurement update consists in updating the estimated distribution of the state based in the measurements, distribution of the measurement noise and the predicted distribution of the state. An efficient algorithm for performing circular filtering is present by the authors of [16], [29] [20].

Consider the following model and measurement equations:

$$\begin{aligned} \theta_{k+1} &= a(\theta_k) + \omega_k, & k \geq 0 \\ z_k &= h(\theta_k) + v_k, & k \geq 0, \end{aligned} \quad (3.12)$$

where $\theta_k \in S^1$ is the state at a timestep k , ω_k is the process noise and v_k is the measurement noise, both assumed to be circular distributed.

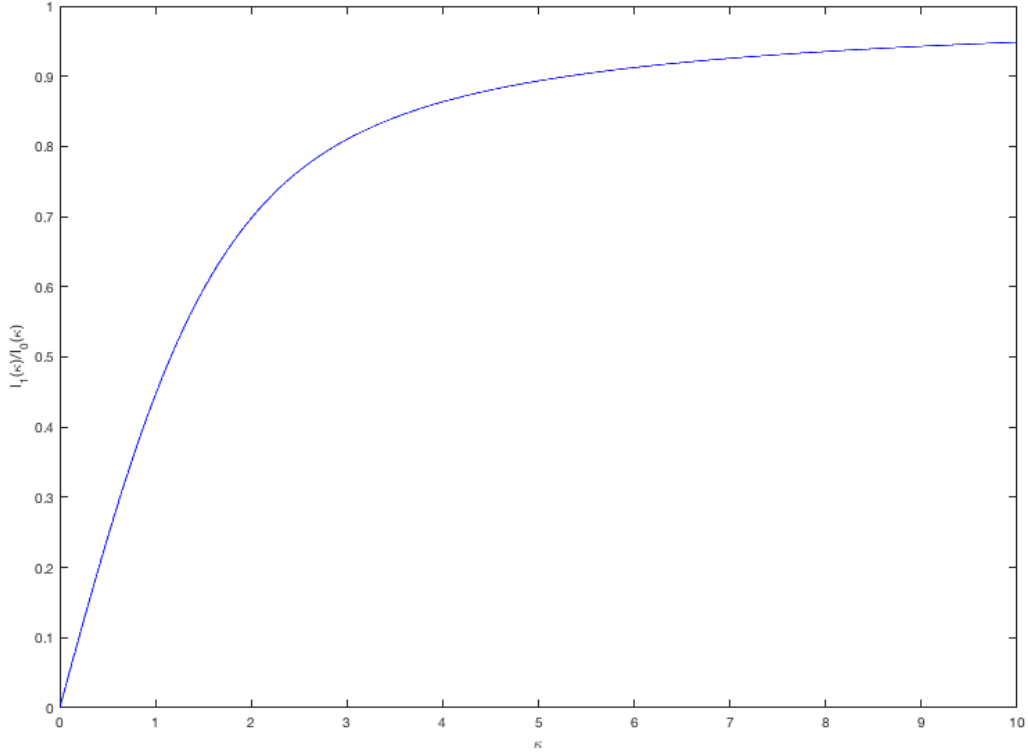


Figure 3.1: Bessel ratio $\frac{I_1(\kappa)}{I_0(\kappa)}$ plotted using the libDirectional toolbox.

To illustrate the prediction stage consider θ_k is WN-distributed with parameters μ_k and σ_k , and that ω_k is an additive also WN-distributed noise with parameters μ_{ω_k} and σ_{ω_k} . The prediction consists at first in approximating the estimated WN density of the current state deterministically with a wrapped Dirac mixture to propagate each component through the system function $a(\cdot)$. Then, the resulting WD distribution is approximated with a WN one by the equations (3.10) and (3.11). Afterwards, the noise ω_k is added by calculating the convolution and result is presented. The algorithm proposed by [26] is described below.

Algorithm 4: Prediction stage on Circular Filtering

Start with $\mu_0^e, \sigma_0^e, \mu_{\omega_k}, \sigma_{\omega_k}$, and the system function $a(\cdot)$. At every time instant $k \geq 0$ compute:

1) Dirac approximation:

$$\alpha = \arccos\left(\frac{3}{2} \exp\left(-\frac{(\sigma_k^e)^2}{2}\right) - \frac{1}{2}\right);$$

2) Application of system function:

$$\beta_1 = a(\mu_k^e - \alpha);$$

$$\beta_2 = a(\mu_k^e);$$

$$\beta_3 = a(\mu_k^e + \alpha);$$

3) Conversion of Dirac components back to WN:

$$\mu = \text{atan2}\left(\sum_{j=1}^3 \sin(\beta_j), \sum_{j=1}^3 \cos(\beta_j)\right);$$

$$\sigma = \sqrt{-2 \log\left(\frac{1}{3} \sum_{j=1}^3 \cos(\beta_j - \mu)\right)};$$

4) Convolution with noise:

$$\mu_k^p = (\mu + \mu_{\omega_k}) \bmod 2\pi;$$

$$\sigma_k^p = \sqrt{\sigma^2 + \sigma_{\omega_k}^2};$$

For the measurement, the nonlinear case is presented in [29] which 3 methods for recursive nonlinear measurement update are presented and their performances are compared. For the sake of clearance and simplicity, we will only present the algorithm for the linear measurement update, but the logic sticks to the nonlinear case with a few assumptions. Therefore, consider the following measurement model:

$$\hat{z}_k = \theta_k + v_k.$$

With measurement \hat{z}_k , state θ_k and additive WN-distributed noise v_k with parameters μ_{v_k}, σ_{v_k} , just as in [26].

The Bayes' rule states that

$$f(\theta_k | \hat{z}_k) = c f(\hat{z}_k | \theta_k) f(\theta_k),$$

with the normalization constant

$$c = \frac{1}{\int_0^{2\pi} f(\hat{z}_k | \theta_k) f(\theta_k) d\theta_k}.$$

The term $f(\hat{z}_k|\theta_k)$ is the likelihood for additive noise and can be obtained by

$$\begin{aligned}
f(\hat{z}_k|\theta_k) &= \int_0^{2\pi} f(\hat{z}_k, v_k|\theta_k)dv_k \\
&= \int_0^{2\pi} f(\hat{z}_k|\theta_k, v_k)f^v(v_k)dv_k \\
&= \int_0^{2\pi} \delta(\hat{z}_k - \theta_k - v_k)f^v(v_k)dv_k \\
&= f^v(\hat{z}_k - \theta_k).
\end{aligned}$$

Where f^v is the distribution of the additive noise v_k . Thus, the equation for the filtered density is obtained

$$f(\theta_k|\hat{z}_k) = cf^v(\hat{z}_k - \theta_k)f(\theta_k).$$

Therefore, the filtering consists in multiplying the densities $f^v(\hat{z}_k - \theta_k)$ and $f(\theta_k)$ and renormalizing afterwards if necessary. The WN distribution is not closed under multiplication, i.e., the product of two WN-distributed variables is not WN-distributed. Then, an intermediate representation by VM distributions is necessary to perform the multiplication. This operation on VM densities is described in [27]. An algorithm for the measurement update is described in algorithm 5, where the *wnToVonMises* and *vonMisesToWn* functions can be either implemented via moment matching (indirect conversion) or by the algorithm presented in [26] for direct conversion between WN and VM distributions.

Algorithm 5: Measurement Update on Circular Filtering

Start with $\mu_0^e, \sigma_0^e, \mu_{v_k}, \sigma_{v_k}$, and the measurement z_0 . At every time instant $k \geq 0$ compute:

1) Shift f^v by measurement:

$$\begin{aligned}\tilde{\mu}_{v_k} &= (\hat{z}_k - \mu_{v_k}) \bmod 2\pi; \\ \tilde{\sigma}_{v_k} &= \sigma_{v_k};\end{aligned}$$

2) Convert to VM distribution:

$$\begin{aligned}\mu_1, \kappa_1 &= wnToVonMises(\mu_k^p, \sigma_k^p); \\ \mu_2, \kappa_2 &= wnToVonMises(\tilde{\mu}_{v_k}, \tilde{\sigma}_{v_k});\end{aligned}$$

3) Multiplication of densities:

$$\begin{aligned}C &= \kappa_1 \cos \mu_1 + \kappa_2 \cos \mu_2; \\ S &= \kappa_1 \sin \mu_1 + \kappa_2 \sin \mu_2; \\ \mu &= \text{atan2}(S, C); \\ \kappa &= \sqrt{S^2 + C^2};\end{aligned}$$

4) Convert back to WN distribution:

$$\mu_k^e, \sigma_k^e = \text{vonMisesToWn}(\mu, \kappa);$$

Chapter 4

Direction of Arrival

Many applications use an array of sensors to estimate the position of wave emitting sources. Those vary from acoustic localization to high precision medical equipment [4]. A DOA estimator is a strong candidate as a measurement source for providing angular measurements in order to a mobile robot perform indoor tracking. In this chapter, an introduction to direction of arrival (DOA) techniques will be presented by analyzing experiments in recent literature, and it's use in a real indoor tracking situation will be evaluated.

4.1 Uniform Linear Array

Since the main objective is to develop a sensor to be fused with a robot to provide angular measurements, the size and complexity of the DOA estimator have to be taken in consideration. A complex but time consuming algorithm is not suitable for real-time estimation and should be avoided in implementation. In addition, if the array or the processor is too large it can compromise mobility of the robot and act as a limiting factor in tracking. Therefore, the kind of array that will be of interest is one developed for embedded systems with a small number of sensors.

In [1] a low cost embedded system capable of estimating the DOA of an acoustic source is developed. A few approximations are made in terms of the distance of the acoustic source (that will be our pedestrian) to the sensors, the number of incident signals for each sensor, and electromagnetic coupling between transducers and electric channels in amplification and filtering. First, it is assumed that the number of incident signals is finite, which leads to a unique solution. In addition, in order to consider the acoustic signals as plane waves, the distance between the acoustic source and the sensors should be 15 times the distance d between those [1]. At last, it is assumed that the electrical channels for filtering and amplification and the transducers are identical and there is no electromagnetic coupling between them.

It is reinforced the importance of the array configuration, since they allow systems to make adaptive use of the spacial diversity [1], [3]. There are a lot of possible geometries for an array of sensors. The circular geometry would be the most favorable since its resolution is of 2π rad, while the linear array, in the other hand, has a resolution of π , which can lead to ambiguity for some

angles. However, for the sake of simplicity and ease of implementation the uniform linear array was chosen. A uniform linear array consists in N sensors positioned in a straight line with equal distance d from one another. The direction of arrival of the signal is equal to the azimuth angle θ . A representation of this kind of array can be observed in the figure 4.1.

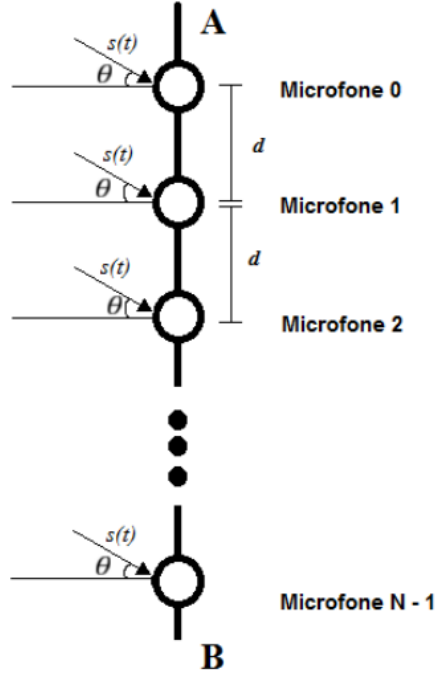


Figure 4.1: Uniform linear array representation (extracted from [1]).

When the assumed plane wave (from a narrow band signal) inflicts over the array, each transducer element will be sensitive to a different delayed version of that wave. Since the first sensor will receive the wave first, there will be a time delay from its received signal and the one from the second sensor. That way, the time delay can be calculated by

$$\Delta t = \frac{\Delta d}{v}.$$

Where Δd is the distance travelled from the first to the second sensor by the wave and v is the propagation velocity from the wavefront. The time delay can be translated into a phase difference ([3]) in terms of the distance of the sensors, the wavelength of the wave and the direction of the source

$$\phi = 2\pi \frac{d \sin(\theta)}{\lambda}.$$

Since the type of array chosen was the uniform linear, there is ambiguity in the estimation for phase differences bigger than π radians in absolute value. Therefore, a condition for the maximum distance of the sensors can be inferred

$$d \leq \frac{\lambda}{2}.$$

That relation is commonly referred as the spacial version of the Nyquist's sampling theorem.

4.2 DOA Estimation Method

The linear array proposed by [1] is composed of only two omnidirectional microphones, with a distance $d = 15\text{cm}$ between them. The acoustic source was defined as a human whistle since it has a narrow band and its central frequency doesn't vary much from person to person. The model can be observed in figure 4.2.

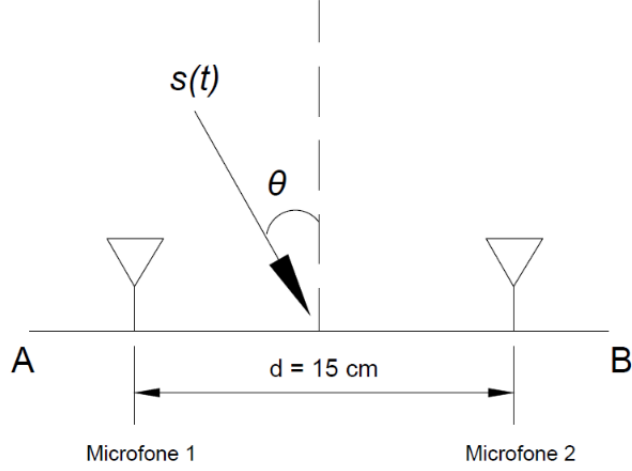


Figure 4.2: Direction of Arrival model considered (extracted from [1]).

The same whistle is received as two signals $m_1(t)$ and $m_2(t)$ with a phase difference that can be expressed as

$$\begin{aligned} m_1(t) &= A_1 s(t) + n(t); \\ m_2(t) &= A_2 s(t - \tau) + n(t). \end{aligned}$$

where $n(t)$ is an additive white gaussian noise (AWGN) and A_1 and A_2 represent the signal gains.

The received signals are subsequently converted into discrete signals via an analog-digital conversion process with sample rate f_{smp} . In [1] the formal treatment to obtain the azimuth angle θ is presented by computing the time delay of the discrete signals and applying the time delay relation previously derived

$$\theta = \sin^{-1}\left(\frac{kv}{d f_{smp}}\right), \quad (4.1)$$

where $v \sim 340$ m/s, $d = 15$ cm. Therefore, a correct estimation of the delay k leads to a correct estimation of the DOA.

4.3 Implementation

The author of [1] proposed a low-budget implementation of a DOA estimator in order to evaluate the theory previously presented. An Arduino Mega was used to receive the microphone

data and perform the analog to digital conversion. Then, the digital data was collected and uploaded to MATLAB to be filtered and estimate the orientation of the source. The sampling frequency was set in 16 KHz for the A/D converter and a cubic spline interpolation was used to increase f_{smp} to 32 KHz for the architecture proposed in the previous section. A resolution of $4,06^\circ$ for the estimated angle was achieved which is not that much considering the hardware limitations.

However, for the purpose of pedestrian tracking, that limitation in resolution has to be considered as an uncertainty about the true direction. In order to make inferences about the probability distribution of the measured angle, a careful study considering measurements of the sensor had to be developed and will be presented on chapters 5 and 6.

4.3.1 Reproducing previous implementation

It would be of interest to reproduce the results obtained by [1] and make further measurements and tests. Also, reproducing the previous implementation would allow us to validate the proposed filters in real time applications. Therefore, a few components were acquired in order to construct the sensors and can be checked in the following list:

- 2x Arduino Nano's V 3.0 ATmega328p;
- 2x External Static Random Access Memories (SRAM) Winbond W25Q128FV;
- 2x sop8 to dip8 adapters;
- 6x 220Ω resistances;
- 6x 330Ω resistances;
- 8x 1.5V batteries.

The prior amplification circuit for the microphones as well as the omnidirectional microphones themselves were obtained from previous projects on DOA estimation, such as [1]. The flash memory adopted and the Arduino type were different from the considered in [1]. The Arduino Nano cheaper and smaller than the Mega one previously implemented, which reduces even more the cost of the embedded sensors. In addition, the memories acquired also differ from the latter case. That way, a direct implementation using the codes from [1] was not possible, since the data acquired by the Arduino was stored in the external memory to provide longer measurement periods. Therefore, a study on the serial peripheral interface (SPI) of the Arduino, specifications of the chosen memory and how to write, read and delete data from it had to be made.

The SPI communication of the Arduino is based on a master/slave configuration. There are three important pins that need to be used to perform SPI communication: MOSI, MISO and SS. The MOSI (master out slave in) reefer to when the data output comes from the master and the slave reads it. Meanwhile, the MISO (master in slave out) the opposite process occurs. The SS is a slave select, since the master can have multiple slaves and it carries the information of which slave is selected to perform the operation. More details on how that process works on Arduino can be

found in [1]. The circuit for the SPI communication and the microphone with its pre amplification circuit can be observed in figures 4.3 and 4.5, respectively. A detail on the connection between the Arduino Nano and the external memory is presented in figure 4.4.

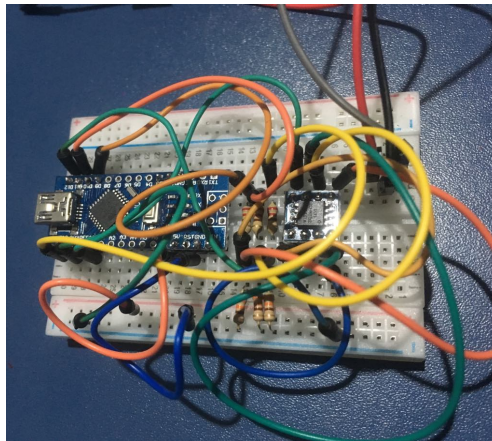


Figure 4.3: Arduino Nano connected to external memory.

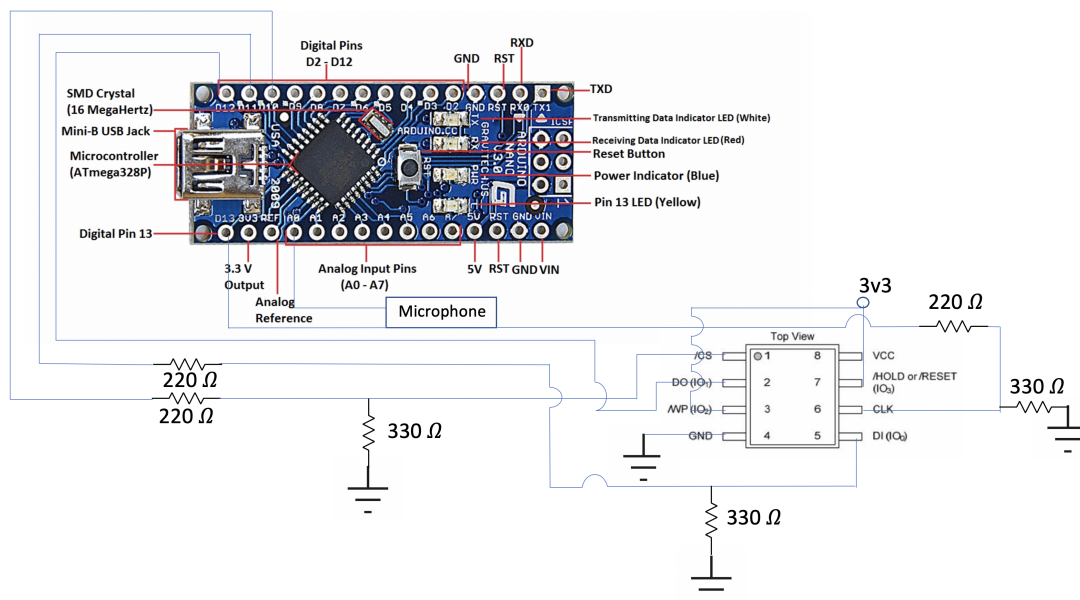


Figure 4.4: Arduino Nano and external memory connection circuit.

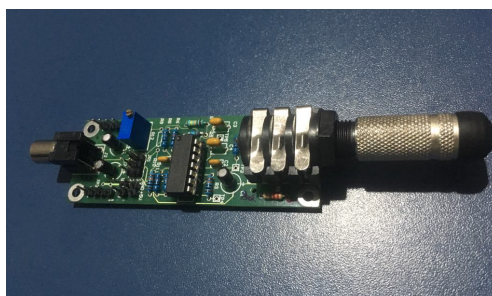


Figure 4.5: Omnidirectional Microphone and its pre amplification circuit.

The external SRAM memory is of vital importance to avoid saturation in the internal memory of the Arduino microprocessor. However, as the memory adopted for implementation is different from the one in [1], the codes for memory access had to be adapted. Due to problems in that adaptation, the sensor could not be finished in time to produce new results and test the filtering algorithms in a real situation. In addition, even if the sensors were operating, there would be a need to study a method to calibrate them and to acquire a ground truth measurement so the results could be validated. For those reasons, the physical implementation of the pedestrian tracking was not covered in this work. Nevertheless, simulations for different filters considering diverse positioning of the sensors were performed in order to provide a solid basis to the actual implementation.

Chapter 5

Simulation Models

5.1 Measurement Equation

As discussed in the previous chapter, an uniform linear array is capable of estimating the direction of arrival of an acoustic source. The acoustic source chosen was a pedestrian whistle for its similarity between different pedestrians and narrow band frequency. That way the pedestrian position can be computed if there is more than one DOA estimator, since one DOA estimator can only provide the pedestrian relative orientation. Consider that two DOA estimators are positioned in a room and provide an angle measurement for a central processing unit (robot). The measurement for each DOA estimator at a time k can be described as follows:

$$\theta_{i,k} = h_i(p_k) + \omega_{i,k}, \quad (5.1)$$

Where p_k is the augmented state vector $[x_k \ y_k \ \dot{x}_k \ \dot{y}_k]^T$, and $\theta_{i,k}$ is the relative angle between the DOA estimator $i \in \{1, 2\}$ and the pedestrian. The noise $\omega_{i,t}$ is WN-distributed with parameters $\mu = 0$ and $\sigma = \sigma_i$. The estimators are stationary and their positions s_1 and s_2 are known exactly.

Our goal is to make some sort of transformation on the angular measurements in order to adequate the measurement equation to be implemented in a linear Kalman filter algorithm. Therefore, the measurements of the two estimators must be transformed into positions measurements in the Euclidean plane. Usually, angular based pedestrian tracking make use of EKF or UKF techniques since the measurement equations have nonlinear functions such as $\text{atan2}(\theta)$. An approach using RFID to model measurement equations is given in [15]. However, a similar approach using circular statistics as the one proposed by [13] can provide a solution that doesn't require nonlinear measurement update and give a correct treatment to the measurement noise.

In order to obtain position measurements at each time step, the noise density of the angular measurements must be deterministically approximated by a wrapped Dirac mixture via moment matching. That can be done by making use of equation 3.8. Then, the resulting WD components placed around the measurement of the respective estimator, can be treated as the uncertainty about the true relative direction of the pedestrian. The problem now is: given a pair of angular measurements and the sensors positions, how can one determine the source location?

By simple geometry, the location can be determined by solving a linear system (since the measurements $\theta_{1,k}$ and $\theta_{2,k}$ are known) considering each coordinate as it follows:

$$\begin{cases} s_{1,x} + a_k \cos(\theta_{1,k}) &= s_{2,x} + b_k \cos(\theta_{2,k}) \\ s_{1,y} + a_k \sin(\theta_{1,k}) &= s_{2,y} + b_k \sin(\theta_{2,k}) \end{cases}$$

where $(s_{1,x}, s_{1,y}) = s_1$ and $(s_{2,x}, s_{2,y}) = s_2$ are the positions in the Euclidean plane for the first and second sensors respectively. A representation of the geometry aforementioned is presented in figure 5.1. Therefore, directional unit vectors for each estimator can be determined

$$u_{1,k} = \begin{bmatrix} \cos(\theta_{1,k}) \\ \sin(\theta_{1,k}) \end{bmatrix}, \quad u_{2,k} = \begin{bmatrix} \cos(\theta_{2,k}) \\ \sin(\theta_{2,k}) \end{bmatrix}.$$

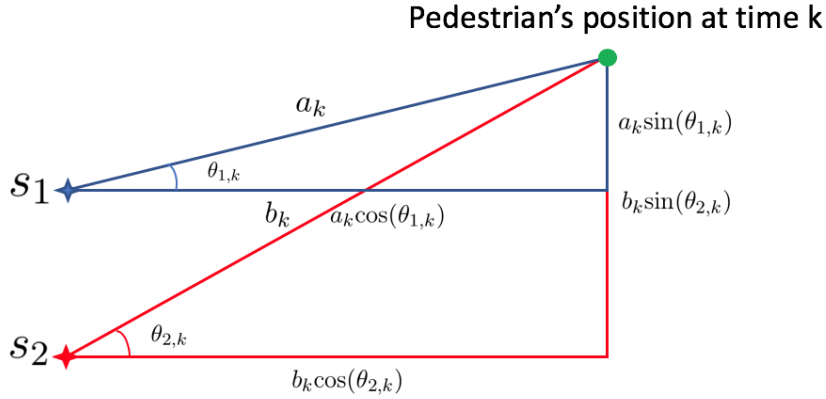


Figure 5.1: Representation of the geometrical strategy to obtain the pedestrian position at time k .

Since there are 3 Dirac components for each $\theta_{i,k}$, there will be 3 directional unit vectors for each true measurement. The computation of $a_k, b_k \in \mathbb{R}$ that satisfy the linear system can be made by defining the following matrix $\mathbf{E} = \begin{bmatrix} -u_{1,k} & u_{2,k} \end{bmatrix}$. Then, a_k and b_k are obtained by

$$\begin{bmatrix} a_k \\ b_k \end{bmatrix} = \mathbf{E}^{-1}(s_1 - s_2).$$

The joined measurement z_k can be defined as

$$z_k := s_1 + a_k u_{1,k} = s_2 + b_k u_{2,k}, \quad (5.2)$$

and its distribution can be obtained by

$$\begin{aligned} f(z_k) &= \int_0^{2\pi} \int_0^{2\pi} f(z, \theta_{1,k}, \theta_{2,k}) d\theta_{1,k} d\theta_{2,k} \\ &= \int_0^{2\pi} \int_0^{2\pi} f(z|\theta_{1,k}, \theta_{2,k}) f(\theta_{1,k}, \theta_{2,k}) d\theta_{1,k} d\theta_{2,k}. \end{aligned}$$

Since z_k is a position measurement, its density should to be approximated by a gaussian distribution. In order to perform such approximation, we approximate $f(\theta_{1,k}, \theta_{2,k})$ by a mixture of Dirac delta components. For each of the 3 possible matrices $u_{1,k}$ and $u_{2,k}$, we compute all the nine possible values for z_k for each pair $(u_{1,k}, u_{2,k})$ by equation 5.2. The mean of this samples is taken as our joined measurement z_k and their empirical covariance as our predicted uncertainty of the joined measurement R_k [13].

By this approach the circular nature of the DOA estimator noise is taken into count for the calculations of z_k and R_k by assuming it's WN-distributed. However, for the measured position the traditional Gaussian model is preserved. The position measurements obtained from the previous angular ones, by the procedure described above, allow a new formulation for the measurement equation:

$$z_k = Hp_k + v_k. \quad (5.3)$$

Where $v_k \sim \mathcal{N}(0, R_k)$ and H is the matrix defined bellow

$$H = \begin{bmatrix} 1 & 0 & 0 & 0 \\ 0 & 1 & 0 & 0 \end{bmatrix}.$$

5.2 Pedestrian Motion

5.2.1 Lavegin Model

In [30], pedestrian indoor tracking based on the time difference of arrival (TDOA) of an acoustic source is presented. In addition, a model based in a Lavegin process to represent pedestrian motion is considered as the system equation. The results obtained by assuming this model in [30] and [15] support its use for pedestrian position estimation and tracking. A Lavegin process for the x coordinate is specified by $\frac{d^2x}{dt^2} + \beta_x \frac{dx}{dt} = F_x$ [30], with β_x the rate constant and F_x a thermal excitation process that will be considered a gaussian noise n_x . A description for a discrete process in the Cartesian plane is given bellow:

$$\begin{aligned} x_{k+1} &= x_k + \Delta T \dot{x}_k \\ y_{k+1} &= y_k + \Delta T \dot{y}_k \\ \dot{x}_{k+1} &= a_s \dot{x}_k + b_s n_x \\ \dot{y}_{k+1} &= a_s \dot{y}_k + b_s n_y. \end{aligned} \quad (5.4)$$

The parameter ΔT is the time-step, $a_s = \exp(-\beta_s \Delta T)$, and $b_s = \bar{v}_s \sqrt{1 - a_s^2}$. Also, the parameter \bar{v}_s is the steady state root-mean-square velocity and β_s is the former mentioned rate constant. In addition, is taken into consideration that the movements in each axis are independent [30]. The noise n_k is assumed to be normally distributed with null mean and covariance Q , i.e., $n_k \sim N(0, Q)$, where

$$n_k = \begin{bmatrix} 0 \\ 0 \\ n_x \\ n_y \end{bmatrix} \quad \text{and} \quad Q = \begin{bmatrix} 0 & 0 & 0 & 0 \\ 0 & 0 & 0 & 0 \\ 0 & 0 & b_s^2 & 0 \\ 0 & 0 & 0 & b_s^2 \end{bmatrix}.$$

A space state equation can be described by the augmented vector $col(x_k, y_k, \dot{x}_k, \dot{y}_k)$ as described bellow:

$$x_{k+1} = Fx_k + n_k, \quad (5.5)$$

where

$$F = \begin{bmatrix} 1 & 0 & \Delta T & 0 \\ 0 & 1 & 0 & \Delta T \\ 0 & 0 & a_s & 0 \\ 0 & 0 & 0 & a_s \end{bmatrix}.$$

Equations 5.5 and 5.3 a traditional Kalman filter approach can be used, not requiring nonlinear state estimation as it did in [15].

5.2.2 Constant Velocity Model

The second model is also a constant velocity model, but a simpler one, since the pedestrian is assumed to cross the room in a straight line. Simulations with a simpler model should provide good performances and can be useful to make comparisons to the Lavegin ones. We will address this second model as the constant velocity model, and its equations of motion are described bellow [9].

$$p_{k+1} = Ap_k + \omega_k,$$

where $p_k = [x_k, y_k, \dot{x}_k, \dot{y}_k]^T$ is the augmented state vector, $\omega_k \sim \mathcal{N}(0, Q)$ is the process gaussian noise and the matrix A is defined as

$$A = \begin{bmatrix} 1 & 0 & \Delta T & 0 \\ 0 & 1 & 0 & \Delta T \\ 0 & 0 & 1 & 0 \\ 0 & 0 & 0 & 1 \end{bmatrix}.$$

A simple diagram is presented for the linear Kalman filter operation in the constant velocity model in figure 5.2. The diagram is equivalent for the Lavegin model.

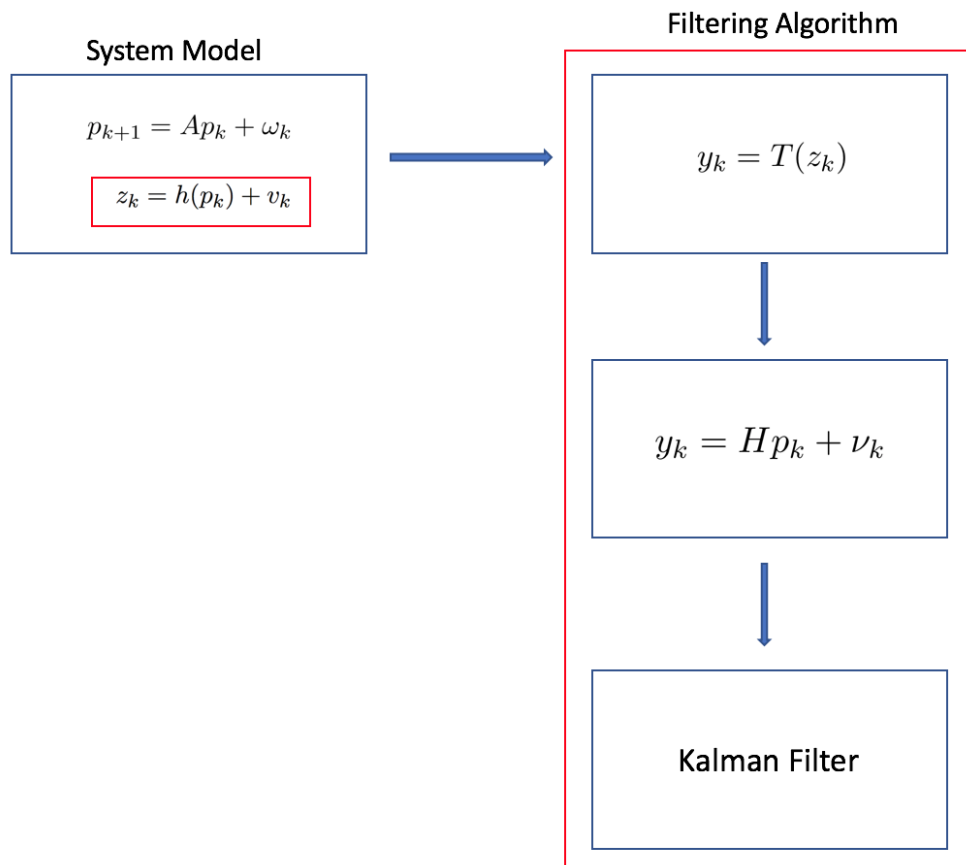


Figure 5.2: Simple diagram is presented for the linear Kalman filter operation in the constant velocity model.

Chapter 6

Simulation Results

6.1 Angular Distribution

In order to evaluate the performance of the presented filter in chapter 5 for pedestrian tracking, first it had to be made a study related to the distribution of the angular measurements acquired by the DOA estimators. In [1], after the implementation of the proposed sensor a few tests were performed to evaluate the similarity of the measured azimuths to the real direction. That way a couple of histograms could be plotted considering the frequency of occurrence of each angle. Since we are interested in circular distributions to describe the probability of the angular measurements, an attempt to fit the histograms presented in [1] in some of the previously discussed circular p.d.f.s has been made.

The choice of which circular distribution to fit the histograms was made considering what has already been approached in the literature and computational effort. Speaker tracking with particle filters assuming Von Mises distributions for the measurements was presented in [5]. Since working with VM distributions requires the computation of Bessel functions and ratios, it was preferred to assume that the measurements would be WN distributed. The figure 6.1 shows the wrapped distributions obtained for different angular measurements.

Another possible representation for those distributions that can provide better visualization is presented in figure 6.2. The parameters of each resulting distribution associated with its measured angle can be observed in table 6.1.

Angle ($^{\circ}$)	Angle (rad)	μ	σ
0	0	6.280	0.0629
30	0.524	0.442	0.143
-30	5.759	5.832	0.114
40	0.698	0.463	0.4368

Table 6.1: Comparison of the WN parameters obtained for different angles.

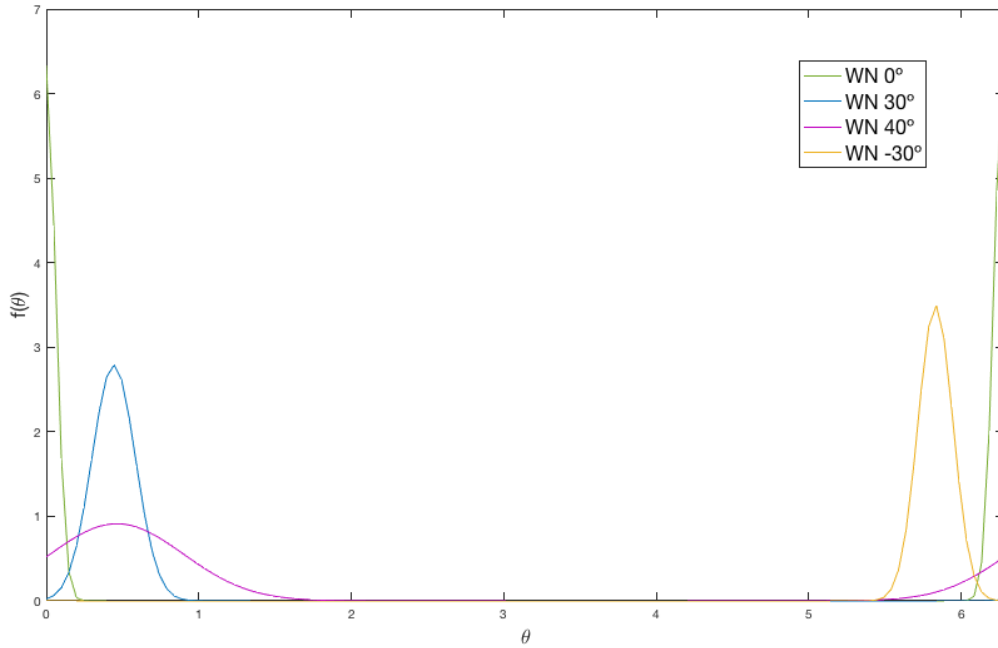


Figure 6.1: Wrapped Normal approximations for measured angles 30° , -30° , 0° and 40° .

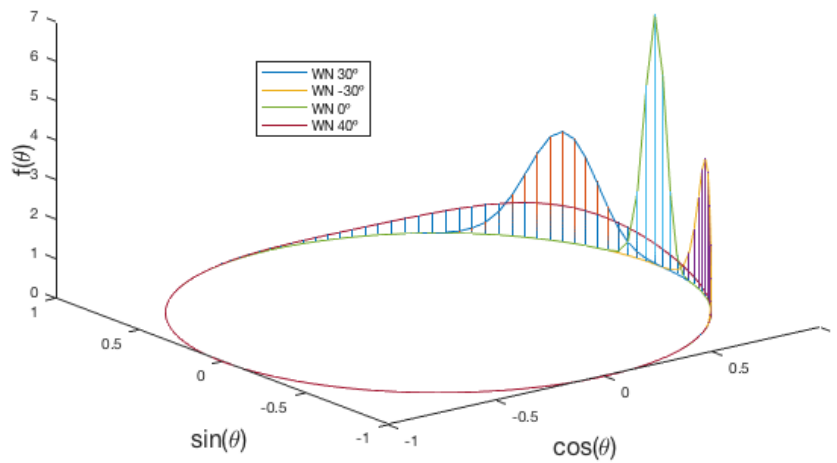


Figure 6.2: Three-dimensional representation of Wrapped Normal approximations for measured angles 30° , -30° , 0° and 40° .

The first point to be noticed in figures 6.1 and 6.2 is that the mean direction of some estimated angles is very close to the actual direction of the acoustic source. Since the representation is made in the interval $[0, 2\pi]$, the negative values for angular data are presented as their equivalent positive angles, as can be observed for the -30° curve. Nevertheless, by the values presented in table 6.1,

the spread of the curves are not that alike so we can make an inference about its value for any given measurement. The uncertainty about a measurement depends on the actual orientation of the source, i.e., for angles within a certain range the spread of the equivalent p.d.f. appear to be far lower than for angles above that range. That can be observed comparing the WN distributions for $\theta = 0^\circ$ and $\theta = 40^\circ$. That way, the problem consists in determining a value for the parameter σ that can be used in the filtering process as the dispersion presented in each angular measurement.

There are a couple approaches to deal with this issue. The first one would be to create a list of angles and consider the different p.d.f.s for each one. The choice of σ would be according to proximity of the true direction to one of the angles in that list. That way we would work with a noise that its characteristics vary with the source direction. On the other hand, a simpler approach would be to consider that the measurements are within a certain range so that an assumption of a fixed value for σ will result in good approximations for the sensor uncertainty. That assumption is plausible considering the position of the sensor and the path available for the acoustic source to move. That way the environment can guarantee that the source orientation will be within a certain range from the DOA estimator.

Considering aspects such as ease of implementation and correct portrait of the acquired data, the second approach is the main choice in the following simulations. The value of σ is set to 0.25 for the WN distributions of each measured angle in order to consider a reasonable uncertainty for the pedestrian estimated direction.

6.2 Environment

In order to evaluate the performance of the Kalman filter described in algorithm 1, and its nonlinear versions described in algorithms 2 and 3 for pedestrian indoor tracking, a simulated room environment can be considered. The room dimensions are 7×7 m and the route of the pedestrian set to be a straight line vertically crossing the room. A representation in the Cartesian plane of the environment and pedestrian route is presented in figure 6.3.

6.3 Linear Kalman Filter Approach

This section aims to apply the transformation proposed in chapter 5 for the measurement equation in order to implement a traditional Kalman filter. In section 6.1, a treatment for the estimated angular measurement of the sensor has been presented so an inference about the σ parameter of the associated WN distribution could be made. However, before the actual filter implementation, a careful analysis of the transformation of angular measurements to pedestrian positions according to position and distance between sensors has to be made.

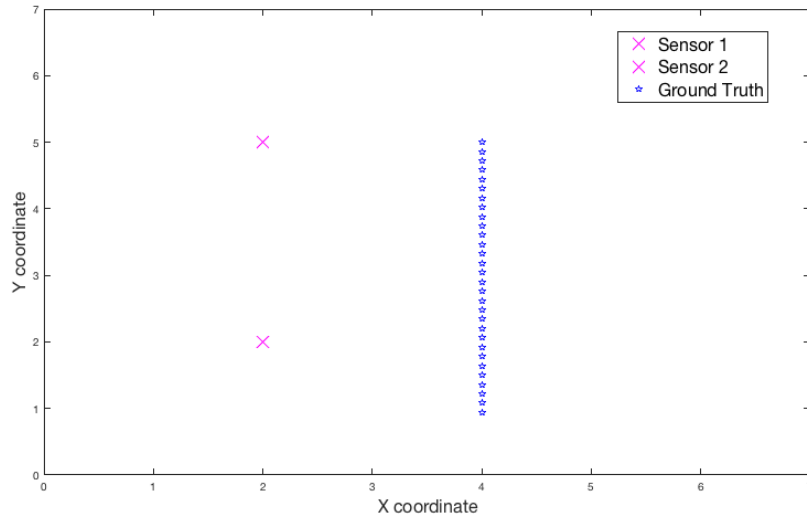


Figure 6.3: Room with dimensions 7X7 and positioned sensors.

6.3.1 Positioning the sensors

The measurements of the DOA sensors are angles referring to the orientation of the source. However, a transformation of those angular measurements considering their uncertainty to position measurements with Gaussian noise was proposed in chapter 5. Therefore, in order to validate the measurements provided by that method, a few simulations were run out to verify how the position of the sensors and distance between them interfere with the resulting measurements. The most relevant results can be observed in figures 6.4 to 6.7.

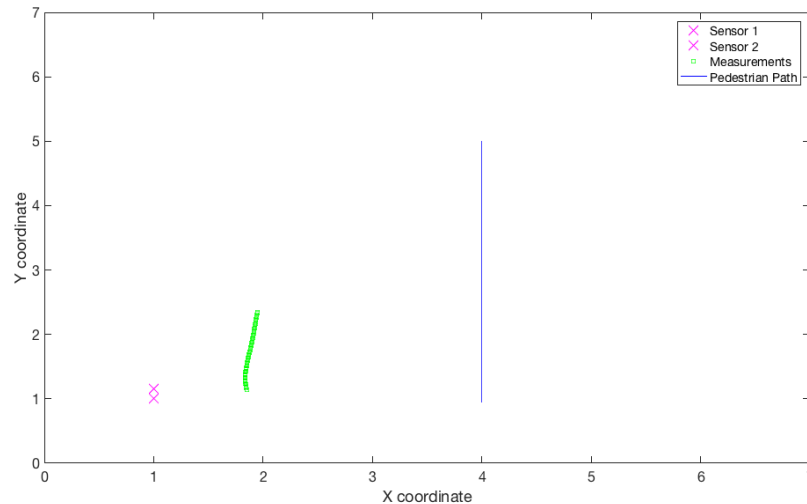


Figure 6.4: Measurements for sensor 1 at (1,1.15) and sensor 2 at (1,1).

From figure 6.4 an immediate problem urges: if the sensors are too close to one another, the angular measurements from both sensors are also too close and the result is similar as if we

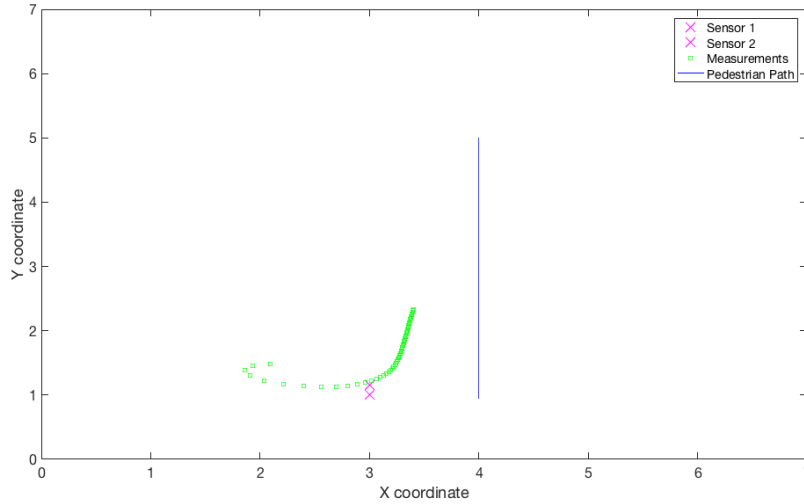


Figure 6.5: Measurements for sensor 1 at (3,1.15) and sensor 2 at (3,1).

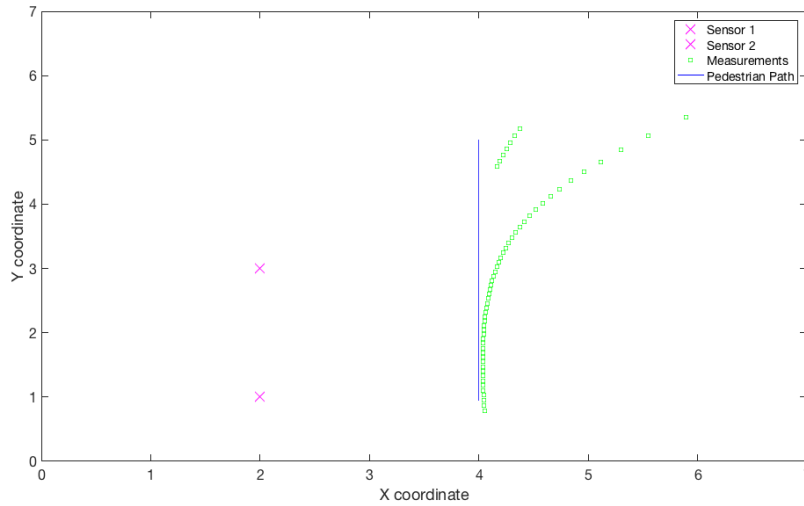


Figure 6.6: Measurements for sensor 1 at (2,3) and sensor 2 at (2,1).

had only one sensor. For one sensor only, since there is an absence of distance measurement, the sensor cannot differ if the pedestrian is close walking at a low speed or distant walking at a fast one, resulting in the observed measurements for position. Also, when the Dirac components of the approximated angular distributions are too close, as illustrated in figure 6.8, the position measurements tend to be outliers. That limitation persists even if the sensors are put closer to the pedestrian, actually the measurements get even worse, as illustrated by 6.5.

The solution then would be to increase the distance between the sensors, in order to work with considerably different angles for each sensor. With a distance of 2 meters between them the resulting measurements already improved as can be seen on figure 6.6. Nevertheless, a portion of the pedestrian path yields bad measurement estimates for the pedestrian true position. Increasing the distance to 4m provided measurements that are really close to the actual path. The results for

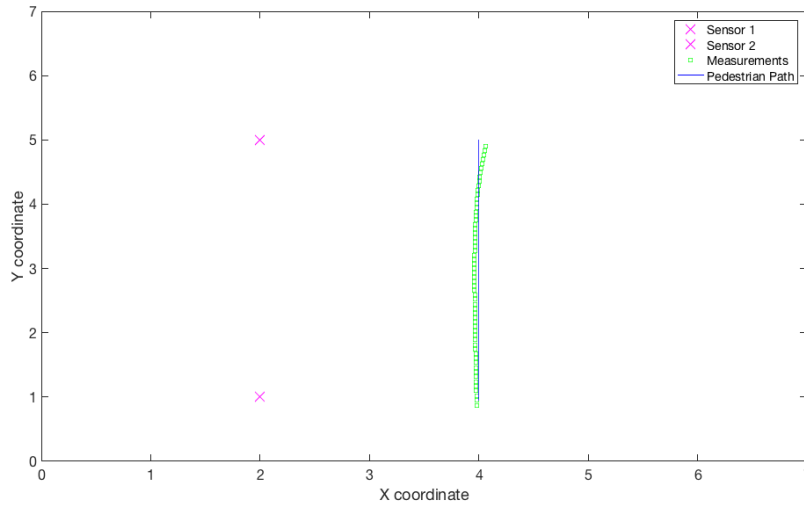


Figure 6.7: Measurements for sensor 1 at (2,5) and sensor 2 at (2,1).

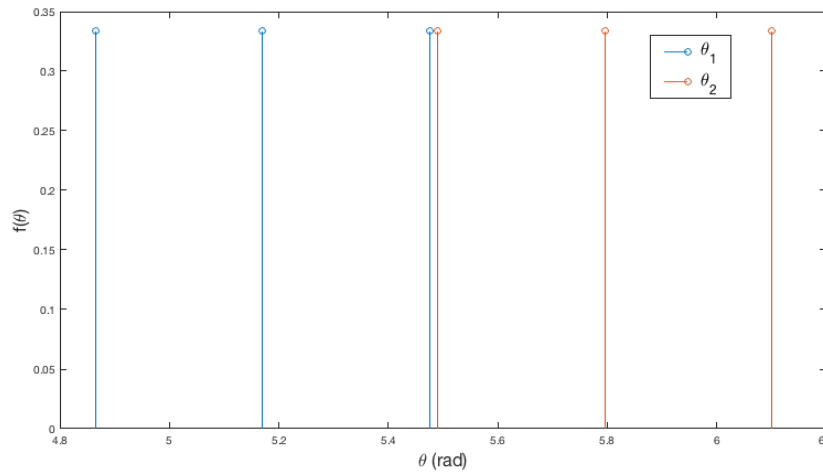


Figure 6.8: Dirac components for two measured angles.

a distance of 4m between sensors can be observed in figure 6.7.

Therefore, the initial objective that was to implement the sensors in a mobile robot so it could perform the tracking of the moving source (pedestrian) is an impossibility for this kind of measurements, since the distance between the sensors would be far superior to the robot dimensions. The following simulations considered then that exists a wireless communication between the robot and sensors and the measured angles are transmitted in real time for the processing unit (robot). The problems related to the links such as time delays, package losses and synchronism are not on the scope of this work, despite being limitations for the filtering process.

6.3.2 Filter Performance

The performance of the proposed filter will be evaluated in terms of the root mean square error (RMSE) and is defined by:

$$RMSE = \sqrt{\frac{\sum_{n=1}^N |\hat{P}_n - P_n|^2}{N}}$$

where \hat{P}_n is the estimated pedestrian position by the filter and P_n is the true position at a time n .

Two different models, introduced in chapter 5, were considered for the simulation and the results of the simulation for both models with different conditions is presented from figure ?? to 6.10.

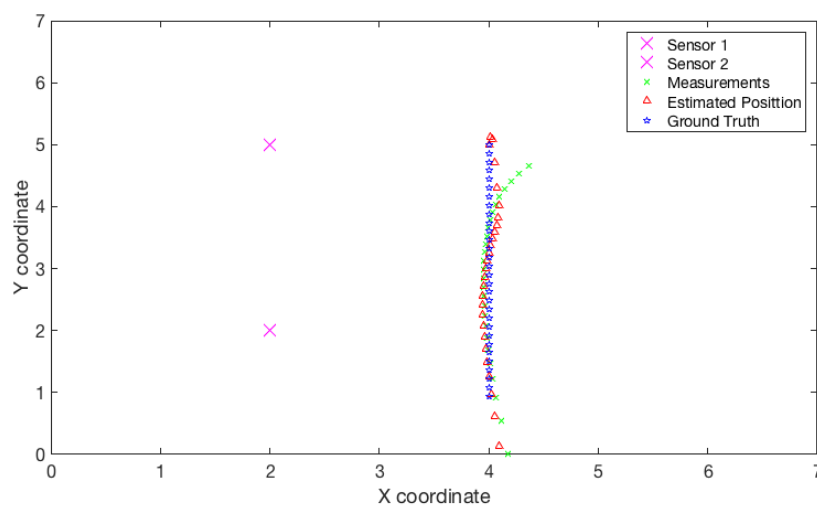


Figure 6.9: State estimation of the pedestrian position with fixed R, linear Kalman filter and Constant Velocity model.

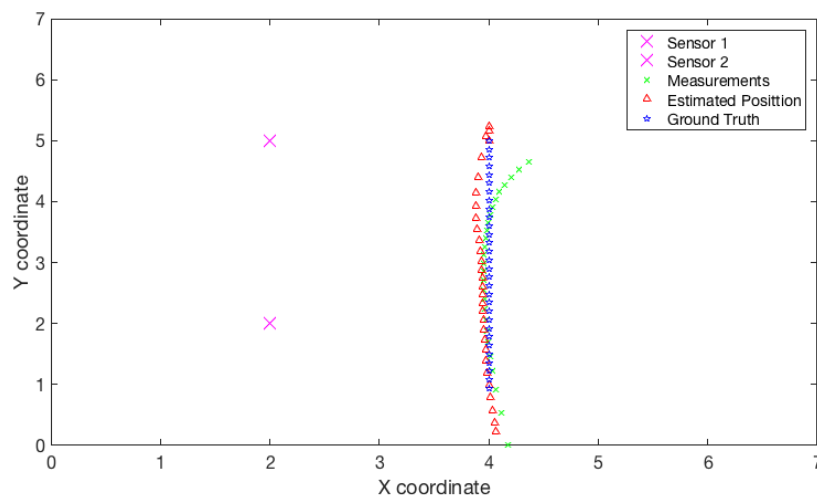


Figure 6.10: State estimation of the pedestrian position with varying R, linear Kalman filter and Constant Velocity model.

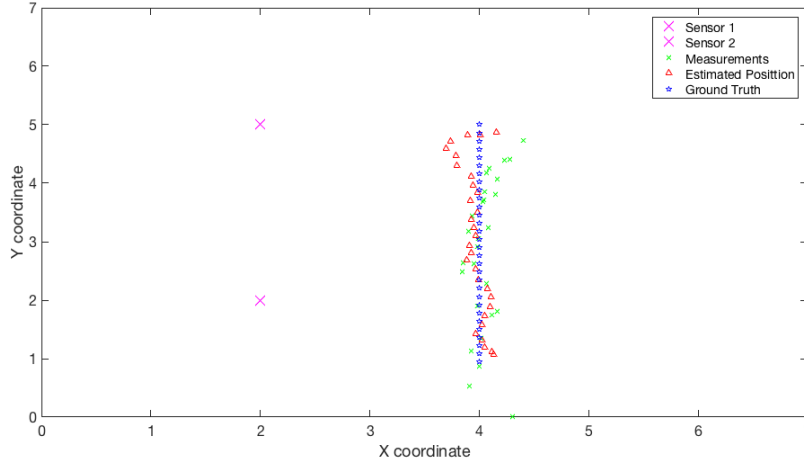


Figure 6.11: State estimation of the pedestrian position with linear Kalman filter and Lavegin model.

The estimation results for the constant velocity model can be observed in figures 6.9 and 6.10. This model seems to describe well the pedestrian walking a straight line at constant velocity, which yield reasonably accurate results for the pedestrian position. The case presented in figure 6.9 considers that the covariance matrix R for the measurements is the same during the whole filtering process, in that case the RMSE for the estimated position is 60.11cm. That might be a surprising result considering that a visually figure 6.9 seem to describe well the motion of the pedestrian. So how can the RMSE be so high? Well that can be explained considering the outlier points mentioned because of proximity between Dirac components. Even if the angular measurements θ_1 and θ_2 are not that close, when their WN distributions are matched to Dirac components, if there is a pair of those components that is too close, the estimated position for that pair tend to be completely different from the actual position. Those measurements can produce wrong estimated positions by the filter that are being considered in the RMSE calculation.

For the result presented in figure 6.10 the noise covariance matrix for the measurements R is considered as stated in chapter 5, i.e., by taking the covariance of the possible values for the measurement. For this scenario the RMSE obtained for the estimated positions is around 39.7cm in contrast to a RMSE of 72.23cm for the measurements. This improvement of almost 50% in the RMSE of the measurements for a σ factor of 0.25 indicates that the filtering algorithm can provide good approximations for uncertain angular measurements. However, in terms of actual pedestrian tracking, an RMSE of 39.7cm is still high when compared to other approaches such as in [15].

For the Lavegin model, the linear Kalman filter still provides a good performance when considering the transformation detailed in chapter 5. Figure 6.11 presents its estimations for pedestrian position. Considering that the Lavegin model is more complex than the constant velocity one, it should describe more accurately the motion of a real pedestrian, therefore it should be adopted for physical implementations. The RMSE for the estimated position was around 24.17cm for a measurement RMSE of 72.39cm, which is better than the constant velocity case.

6.4 EKF and UKF Approaches

In order to compare the obtained results for traditional Kalman filtering to more sophisticated filtering techniques, an implementation of the same problem for a EKF and UKF filters was approached. For this kind of approach, the measurement equation would be different than the presented in chapter 5 and is described at it follows:

$$z_k = h(p_k) + v_k, \quad (6.1)$$

where p_k is the pedestrian position (x_k, y_k) at instant k , v_k is a gaussian noise with mean 0 and covariance R (assumed constant). The function $h(x_k, y_k)$ is given by

$$h(x_k, y_k) = \begin{bmatrix} \text{atan2}(y_k - s1_y, x_k - s1_x) \\ \text{atan2}(y_k - s2_y, x_k - s2_x) \end{bmatrix}. \quad (6.2)$$

Where $(s1_x, s1_y)$ and $(s2_x, s2_y)$ are the known positions of the first and second sensor respectively. Therefore, for the EKF implementation, the Jacobian of $h(x_k, y_k)$ is given by

$$\frac{\partial h(x_k, y_k)}{\partial p_k} = \begin{bmatrix} -\frac{y_k - s1_y}{(x_k - s1_x)^2 + (y_k - s1_y)^2} & \frac{x_k - s1_x}{(x_k - s1_x)^2 + (y_k - s1_y)^2} \\ -\frac{y_k - s2_y}{(x_k - s2_x)^2 + (y_k - s2_y)^2} & \frac{x_k - s2_x}{(x_k - s2_x)^2 + (y_k - s2_y)^2} \end{bmatrix}. \quad (6.3)$$

The linear approximation of $h(x_k, y_k)$ is performed at each new predicted position, since they are the operation points for the system at each time step. Both the Lavegin and constant velocity models are considered for EKF and UKF evaluations and their performances can be visualized at figures 6.12 and 6.15.

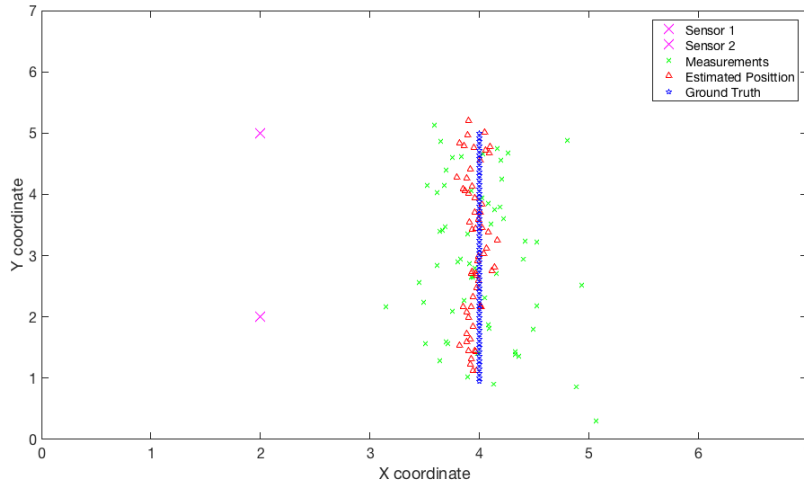


Figure 6.12: State estimation of the pedestrian position with EKF and Lavegin model.

From figures 6.12 and 6.13 it can be observed that the EKF filter performs reasonably well with only angular measurements. For the straight line case the constant velocity model assumption does not provides better results than the Lavegin one. The RMSE in the estimated position is around 27.54cm for the constant velocity model given a measurement RMSE of 37.29cm. On the other

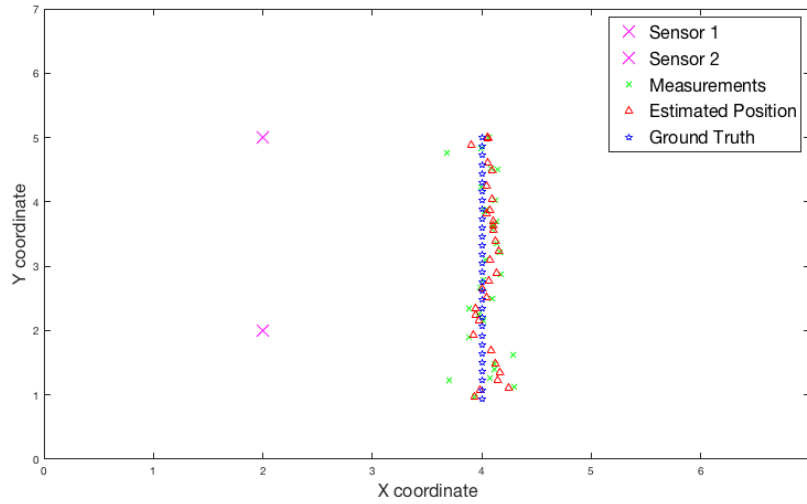


Figure 6.13: State estimation of the pedestrian position with EKF and Constant Velocity model.

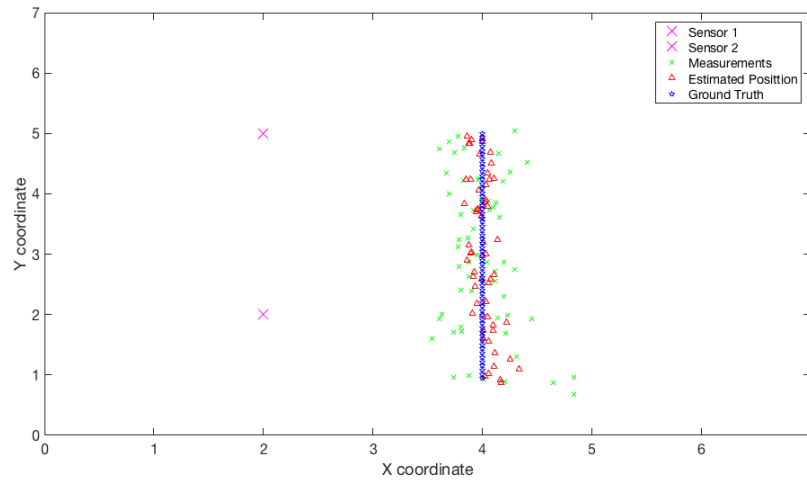


Figure 6.14: State estimation of the pedestrian position with UKF and Lavegin model.

hand, for the Lavegin model a estimated position RMSE of 32.03cm for measurement RMSE of 48.95cm which is a similar performance considering the position RMSE even for a higher uncertainty on the measurements. That way, the Lavegin model provides similar performance results given a higher RMSE on measurements, which speaks in favor of its use in a physical implementation. The Q matrices have been tuned heuristically in order to obtain valid approximations. Nevertheless, since its not our main focus to obtain the best possible estimate for the EKF filter, the RMSE of the constant velocity model already serves the purpose for comparing with the designed traditional Kalman filter of the previous section. The Q matrices for the Lavegin and

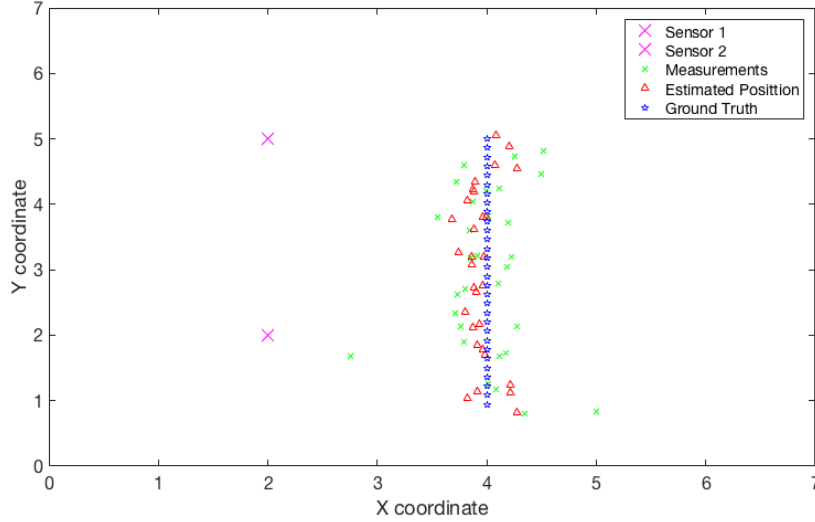


Figure 6.15: State estimation of the pedestrian position with UKF and Constant Velocity model.

constant velocity models in the EKF approach are presented bellow:

$$Q_{\text{Constant Velocity}} = \begin{bmatrix} 0 & 0 & 0 & 0 \\ 0 & 0 & 0 & 0 \\ 0 & 0 & 0.4197 & 0 \\ 0 & 0 & 0 & 0.4197 \end{bmatrix} \quad Q_{\text{Lavegin}} = \begin{bmatrix} 0 & 0 & 0 & 0 \\ 0 & 0 & 0 & 0 \\ 0 & 0 & 0.4460 & 0 \\ 0 & 0 & 0 & 0.4460 \end{bmatrix}$$

The UKF filters performs really similar to the EKF for both models, their performances can be verified in figures 6.15) and 6.14. The RMSE for the UKF estimated position in the constant velocity model is 35.52cm in contrast with an measurement RMSE of 44.43cm. As for the Lavegin model the RMSE of the estimated position was around 32.39cm for ma measurement RMSE of 49.13cm. Hence, the Lavegin model provides better approximations for all the considered filters, presenting itself as a more suitable choice for physical implementations. An optimization of matrix Q values will certainly provide better approximations but, as mentioned before, is not the main focus of this work since those filters were only implemented to validate their use in pedestrian tracking based on the discussed sensor measurements. It's important to point out that just replicating Q matrices values from similar experiments such as [15], where the same model was chosen with only different measurement equations, does not result in similar results, therefore the need for tuning. Therefore, heuristic values for those matrices had to be chosen considering the new situation.

6.5 Comparison of the Filters Performances

The most relevant results from simulations for both models described in the previous sessions, are presented in tables 6.2 and 6.3. Initial comparison suggests that the three filter implementations can perform reasonably good tracking of pedestrians in indoor environments with the presented

sensors. For the straight line motion, the constant velocity model is expected to result in more accurate approximations for simple tuning attempts of the Q matrices, however the Lavegin model provided even better approximations being the main choice for physical implementations. The uncertainties considered for the angular measurements were based on our studies on the histograms provided by [1]. However, the uncertainties considered to the EKF and UKF case seem to be far lower considering the measurements RMSEs due to not dealing with the problems related to the transformation.

For a RMSE of 38.12cm the RMSE of the linear Kalman filter is around 24.5cm, being lower than the EKF equivalent for the constant velocity model. Since the angular uncertainty is not very high, the treatment provided by circular statistics doesn't assure much better estimations than traditional nonlinear Kalman methods. However, when the RMSE for measurements are elevated to 71.2cm the correspondent RMSE of the EKF is 48.86cm, which is almost 10cm greater than the linear Kalman one. Both results for the low (Linear/EKF A) and high (Linear/EKF B) angular uncertainty cases are presented o table 6.2. On the other hand, the drawbacks caused by large measurement errors when the Dirac components of the possible angle values are too close can lead to really poor approximations for the discussed filter. Therefore, the precision of the tracking is limited by the arrangement of the sensors, a correct modeling of the measurement uncertainty and a careful tuning of the Q covariance matrix, which the latter can yield really poor performance in filtering.

Filter	Estimated RMSE (cm)	Measurement RMSE (cm)
Linear A	39.7	72.23
Linear B	24.5	38.12
EKF B	27.54	37.29
EKF A	48.86	71.2
UKF	35.52	44.43

Table 6.2: Comparison of the RMSEs obtained for the different filter approaches considering the constant velocity model.

Filter	Estimated RMSE (cm)	Measurement RMSE (cm)
Linear	24.17	72.39
EKF	32.03	48.95
UKF	32.39	49.13

Table 6.3: Comparison of the RMSEs obtained for the different filter approaches considering the Lavegin model.

Chapter 7

Concluding remarks

In this work, a performance analysis on filters to improve pedestrian tracking was carried. The problem of determining the uncertainties of the measured angles could be addressed through circular statistics approximations. The transformation of the measured angles to position ones, discussed in chapter 5, results in a viable solution considering a correct treatment of angular uncertainties. Through simulations, we made clear the problems in positioning of the sensors to acquire valid data for the acoustic source true position. The need of distance between sensors requires reevaluation on communication between the its microprocessors and the central unit (robot). In addition, simulations provided insights with respect to position outliers due to close Dirac components in the method provided by [13]. A comparison in the performance of the filters for both presented models shows that a Kalman filter with a correct treatment of angular quantities of the DOA sensors can provide results as good as EKF and UKF filters when the uncertainty is not high. For higher uncertainty levels the linear Kalman filter outperforms EKF providing estimations with lower RMSE. The Lavegin model provides better results for sub-optimal Q matrices, therefore being a suitable model to be considered on indoor pedestrian tracking problems. In conclusion, the filter discussed in chapter 5 considers the circular nature of the measurements and provide a more reliable estimation for the true pedestrian position than sensor measurements only. Even though EKF or UKF approaches can provide good estimations, for higher measurement uncertainties the proposed filter provides better results. Therefore, the proposed filter would be a valid choice for implementation in a real time estimation problem.

7.1 Future Work

A theoretical development and simulations were presented, however the physical implementation of the suggested filter to validate simulation results is yet to be done. Implementation of the filter in a mobile robot and configuring its communication with the Arduino to acquire real time results would be a valuable contribution. In addition, considerations regarding information loss and link failure will provide more accurate results and improved performance of the physical implementation. Also, considerations due to reverberation on the environment and synchronism

of measurements provided by the DOA sensors was not on the scope of this work and presents a valid analysis for future works.

Furthermore, the scenario analyzed in this work only concerns position estimation in the Cartesian plane. The source's location and microphones positions are assumed to be at the same height. However, this assumption places a constraint on the applications. Therefore, a relevant contribution would be a extension of the suggested filtering algorithm to the three dimensional space.

Finally, an extension of the study developed in this work to distributed filtering case is at hand. The task would consist in considering a larger network of sensors combined with multiple processing units that are capable of communicating with each other to provide more accurate estimations.

Bibliography

- [1] TORRES, G. S. *Estimação de direção de chegada de sinal sonoro utilizando arranjo de sensores*. 51 p. Trabalho de Graduação, Universidade de Brasília, 2018.
- [2] MARDIA, K.; JUPP, P. E. *Directional Statistics*. [S.l.]: John Wiley Sons, 2000.
- [3] GONTIJO, A. T. *Estimador de direção de chegada em tempo real com arranjo de microfones*. 127 p. Dissertação de Mestrado, Universidade de Brasília, 2010.
- [4] BRANDSTEIN, M.; WARD, D. *Microphone Arrays: Signal Processing Techniques and Applications*. 1. ed. [S.l.]: Springer-Verlag Berlin Heidelberg, 2001.
- [5] MARKOVIĆ, I.; PETROVIĆ, I. Speaker localization and tracking with a microphone array on a mobile robot using von Mises distribution and particle filtering. *Robotics and Autonomous Systems*, Elsevier B.V., v. 58, n. 11, p. 1185–1196, 2010.
- [6] SONG, T. L.; SPEYER, J. L. A Stochastic Analysis of a Modified Gain Extended Kalman Filter with Applications to Estimation with Bearings Only Measurements. *IEEE Transactions on Automatic Control*, v. 30, n. 10, p. 940–949, 1985.
- [7] ERLANDSSON, T. *Angle-only target tracking*. Bachelor's Thesis, Linköpings universitet, 2007. Disponível em: <<http://www.diva-portal.org/smash/get/diva2:23313/FULLTEXT01.pdf>>.
- [8] FARINA, A. Target tracking with bearings - only measurements. *Signal Processing*, v. 78, n. 1, p. 61–78, 1999.
- [9] RESHMA, A.; ANOOJA, S.; DEEPA, E. G. Bearing Only Tracking using Extended Kalman Filter. *International Journal of Advanced Research in Computer and Communication Engineering*, v. 2, n. 2, p. 1140–1144, 2013.
- [10] SONG, T. L. Observability of target tracking with bearings-only measurements. *IEEE Transactions on Aerospace and Electronic Systems*, v. 32, n. 4, p. 1468–1472, 1996.
- [11] JAMMALAMADAKA, S. R.; SENGUPTA, A. *Topics in Circular Statistics*. [S.l.]: World Scientific Publishing Co. Pte. Ltd., 2001. e20505 p.
- [12] TRAA, J.; SMARAGDIS, P. A Wrapped Kalman Filter for Azimuthal Speaker Tracking. *IEEE Signal Processing Letters*, v. 20, n. 12, p. 1257–1260, 2013.

- [13] GILITSCHENSKI, I.; KURZ, G.; HANEBECK, U. Bearings-only sensor scheduling using circular statistics. *Information Fusion (FUSION)*, 2013, p. 515–521, 2013.
- [14] JULIER, S.; UHLMANN, J.; DURRANT-WHYTE, H. A new approach for filtering nonlinear systems. *Proceedings of 1995 American Control Conference*, v. 3, n. June, p. 1628–1632, 1985.
- [15] SILVA, C. F. *A Performance Analysis of Distributed Filtering Algorithms for Indoor Pedestrian Tracking*. 54 p. Trabalho de Graduação, Universidade de Brasília, 2017.
- [16] KURZ, G. *Karlsruhe Series on Intelligent Sensor-Actuator-Systems: Directional Estimation for Robotic Beating Heart Surgery*. [S.l.]: KIT scientific Publishing, 2015.
- [17] PAULA, F. V.; NASCIMENTO, A. D. C.; AMARAL, G. J. A new extended Cardioid model : an application to wind data. p. 1–30, 2017. Disponível em: <<https://arxiv.org/abs/1712.01824>>.
- [18] TRAN, V. H. et al. Bayesian Inference for Multi-Line Spectra in Linear Sensor Array. *43rd International Conference on Acoustics, Speech and Signal Processing*, p. 4254–4258, 2018.
- [19] KHAE, A.; NAVARRO, W. *Probabilistic Machine Learning for Circular Statistics Models and inference using the Multivariate Generalised Von Mises distribution*. Tese (Doutorado), 2019. Disponível em: <<https://doi.org/10.17863/CAM.26449>>.
- [20] KURZ, G.; GILITSCHENSKI, I.; HANEBECK, U. D. Recursive Bayesian Filtering in Circular State Spaces. 2015. Disponível em: <<https://arxiv.org/abs/1501.05151>>.
- [21] ABRAMOWITZ, M.; STEGUN, I. A. *Handbook of Mathematical Functions: with Formulas, Graphs and Mathematical Tables*. [S.l.]: Dover Publications, 1965. 1046 p.
- [22] AMOS, B. D. E. Computation of Modified Bessel Functions and Their Ratios. *Society*, v. 28, n. 125, p. 239–251, 1974.
- [23] MORETTIN, P. A.; BUSSAB, W. O. *Estatística Básica*. 6. ed. [S.l.]: Editora Saraiva, 2010.
- [24] ROUSSAS, G. G. *An introduction to probability and statistical inference*. [S.l.]: Academic Press, 2007. 515 p.
- [25] SAYED, A. H. *Adaptive Filters*. [S.l.]: John Wiley Sons, 2008.
- [26] KURZ, G.; GILITSCHENSKI, I.; HANEBECK, U. D. Recursive Nonlinear Filtering for Angular Data Based on Circular Distributions. *Proceedings of the 2013 American Control Conference*, 2013.
- [27] AZMANI, M. et al. A recursive fusion filter for angular data. *IEEE International Conference on Robotics and Biomimetics*, IEEE, p. 882–887, 2009.
- [28] KURZ, G. et al. Methods for Deterministic Approximation of Circular Densities Methods for Deterministic Approximation of Circular Densities. *Journal of Advances in Information Fusion*, v. 11, p. 138–156, 2016.

- [29] KURZ, G.; GILITSCHENSKI, I.; HANEBECK, U. D. Nonlinear Measurement Update for Estimation of Angular Systems Based on Circular Distributions. *2014 American Control Conference*, p. 5694–5699, 2014.
- [30] VERMAAK, J.; BLAKE, A. Nonlinear filtering for speaker tracking in noisy and reverberant environments. *Proceedings of IEEE International Conference on Acoustics, Speech, and Signal Processing*, v. 5, p. 3021–3024, 2001.